CrossMark

Recent Advances in Polymer Organic Light-Emitting Diodes (PLED) Using Non-conjugated Polymers as the Emitting Layer and Contrasting Them with Conjugated Counterparts
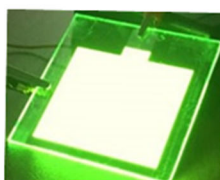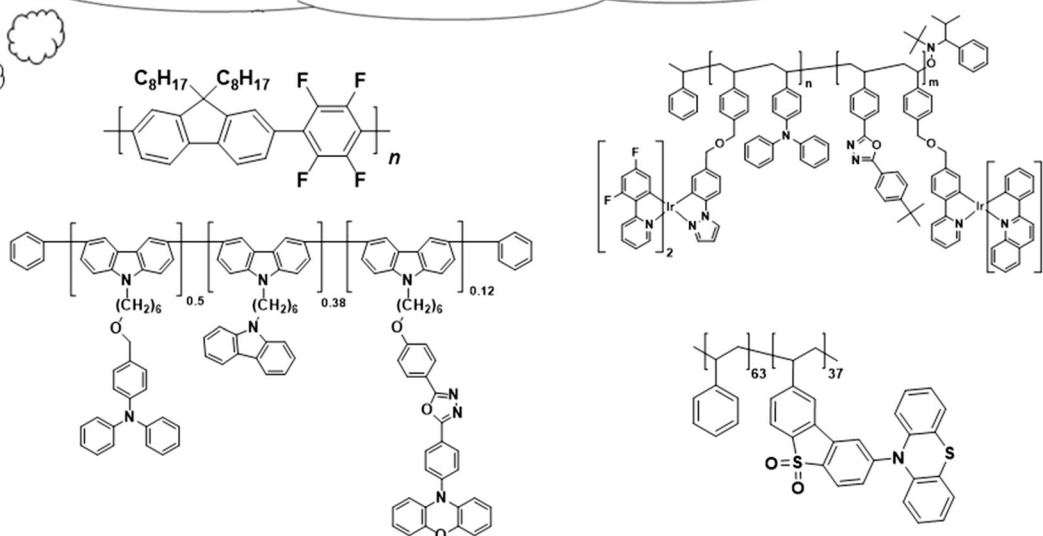
MICHAEL Y. WONG [1,2]

1.—School of Chemistry, University of St. Andrews, St. Andrews, Fife, UK. 2.—e-mail: yw40@st-andrews.ac.uk

Polymer organic light-emitting diodes (PLED) are one of the most studied subjects in flexible electronics thanks to their economical wet fabrication procedure for enhanced price advantage of the product device. In order to optimize PLED efficiency, correlating the polymer structure with the device performance is essential. An important question for the researchers in this field is whether the polymer backbone is conjugated or not as it affects the device performance. In this review, recent advances in non-conjugated polymers employed as the emitting layer in PLED devices are first discussed, followed by their contrast with the conjugated counterparts in terms of polymer synthesis, sample quality, physical properties and device performances. Such comparison between conjugated and non-conjugated polymers for PLED applications is rarely attempted, and; hence, this review shall provide a useful insight of emitting polymers employed in PLEDs.

Recent Advances in Polymer Organic Light-Emitting Diodes (PLED) Using Non-conjugated
Polymers as the Emitting Layer and Contrasting Them with Conjugated Counterparts

6247

Graphical Abstract

INTRODUCTION

Organic light-emitting diodes (OLEDs, see Table SI for abbreviations used in this review) have reached the apex of display technology thanks to a number of their distinctive merits such as excellent image quality and contrast, having a large viewing angle and being light, thin and flexible. Since the pioneering report of an operational OLED device by Tang and VanSlyke in 1987[1] tremendous research from both the academia and industry has been devoted to optimize the device's performance. During the past 30 years, workers in the field have witnessed an enormous enhancement in the device efficiency, escalating from the initial external quantum efficiency (EQE) of 1%[1] to the current state-of-the-art EQE of $>30\%$[2–5] (*without* additional device architecture for enhanced light-outcoupling). Meanwhile, notable OLED companies such as Samsung

and LG have already commercialized OLED televisions, laptops and touchscreens in mobile phones. Furthermore, being an energy-efficient technology, OLED lighting will help alleviate power consumption that at currently about 20% of total electricity consumption is devoted solely to lighting purposes.[6]

Apart from device efficiency, the ease of fabrication also plays an essential role in the marketability of OLED technology, because it reduces the device manufacturing cost. In this regard, the wet process (spin-casting or inkjet printing) is more beneficial than the dry process (vacuum thermal deposition), especially in the case of large-area display devices.[7–9] In the wet fabrication process, materials are dissolved in a suitable organic solvent to form a solution that can be conveniently applied onto the substrate. The solution should possess a certain degree of viscosity, and the resulting film must have

high surface quality and robust morphological stability, all of these can be fulfilled nicely by polymeric materials.[10,11] As a result, polymer OLED (PLED) materials have long been the center of research efforts. The first PLED was reported by Burroughes and co-workers in 1990 when they invented the famous poly(*p*-phenylene vinylene) (PPV, Fig. 1) as a green-yellow emitter, which offered a device EQE of 0.05%.[12] This early emitting polymer was itself intractable, and; therefore, soluble polymer precursor had to be spun-coated on a substrate followed by thermal curing (250°C) under vacuum to generate the polymer. Then, poly[2-methoxy-5-(2-ethylhexyloxy)-1,4-phenylenevinylene] (MEH-PPV, Fig. 1) was developed, which was a soluble derivative of PPV and gave an orange-red device, suggesting the alkoxy substituents at 2- and 5-positions impact both emission colors and solubility of the polymer.[13] Polyfluorene (PFO, Fig. 1) is a classic blue-emitting polymer, which has been intensively studied.[14,15] Finally, poly(*N*-vinylcarbazole) (PVK, Fig. 1) is a very popular hole-transporting layer and host material employed in the emitting layer of OLED devices.[11]

Polymers for PLED applications can be divided into two main classes according to their architecture (Fig. 2). One of them has a conjugated backbone in which the π-electron density in one repeating unit can be delocalized over other units (Fig. 2a). While the conjugated backbone is already functional (charge transport and/or emission) on its own (Fig. 2-a, top), it is sometimes decorated with a pendant electroactive group for acquiring additional properties (Fig. 2a, bottom).[16–18] On the other hand, non-conjugated polymer backbones have repeating units that are electrically isolated from each other. Because the polymer backbone is insulating, it is invariably attached with electroactive groups to impart charge-transporting and/or emissive properties to the polymer (Fig. 2b).[19–21] In this review, recent advances (mainly after 2010) in non-conjugated polymers employed as emitters in PLED devices will be discussed, where they can be divided into three main classes of materials: fluorescent, phosphorescent and thermally activated delayed fluorescent (TADF). Their synthetic parameters such as polymerization method and yield, molecular weight distribution and purity shall be contrasted with those of recently reported conjugated polymers (2011-present). Moreover, the PLED efficiencies and determining factors such as photoluminescence quantum yield (PLQY), glass-transition temperature (T_g, see Table SIII for symbols used in this review), and film surface roughness (R) of these two classes of polymers shall also be contrasted. A literature survey reveals that such systematic comparison between non-conjugated and conjugated PLED polymers is rarely attempted. Therefore, this review shall provide a useful perspective of understanding the similarities and differences between conjugated and non-conjugated polymers for PLED applications.
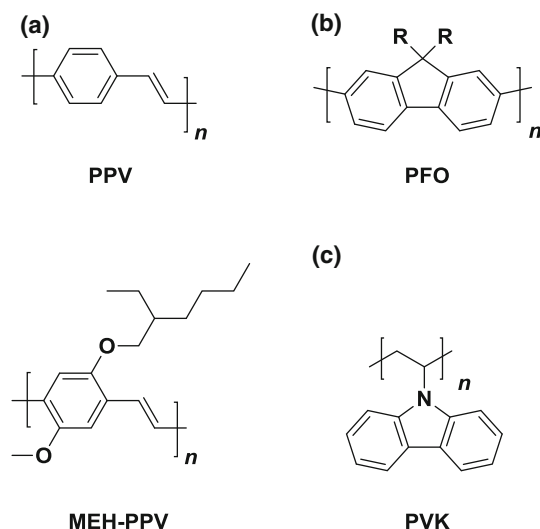

Fig. 1. Chemical structures of PPV and MEH-PPV a), PFO b) and PVK c).

RECENT ADVANCES IN NON-CONJUGATED POLYMERS FOR PLED APPLICATIONS

Phosphorescent Polymers

According to spin statistics, 75% of excitons in OLED devices are triplet in nature whose radiative transition to the ground singlet state is spin-forbidden, and; thus, they are mostly lost as heat.[22] In order to solve this problem, organometallic complexes built with heavy metals such as iridium and platinum are employed as phosphorescent emitters in OLED devices.[6,22,23] The large spin-orbit coupling constants (ζ) of those metals increase the rate of intersystem-crossing (ISC) to shorten phosphorescence lifetime to useful microsecond regimes.[6,22,24] As a result, phosphorescent OLEDs can achieve 100% internal quantum efficiency (IQE) and devices showing stellar external quantum efficiencies (EQEs) of >30% have been reported.[5,25]

Lai et al. prepared a polystyrene functionalized with dendronized iridium(III) phosphor (**DIr-P1**, Fig. 3) for PLED applications.[26] In order to suppress interchromophore interactions, bulky 1,3-bis(2-ethylhexyloxyphenyl)phenyl dendrons were decorated to impose steric hindrance around the central phosphor, which were brought close to one another by the polymer side chain. Phosphor aggregation is particularly detrimental to device efficiency because of enhanced aggregation-caused quenching (ACQ) and triplet-triplet annihilation (TTA).[9] It was found that the dendronized polymer exhibited significantly better photophysical properties than the non-dendronized one (**Ir-P1**, Fig. 3). For example, **DIr-P1** had Φ_{PL} of 61% and 13% in degassed dichloromethane (DCM) solution and neat film, respectively, which were significantly higher than those of **Ir-P1** (Φ_{PL}: 23% in degassed DCM and <1% in neat film), although it was evident that a certain extent of aggregation was still present in the
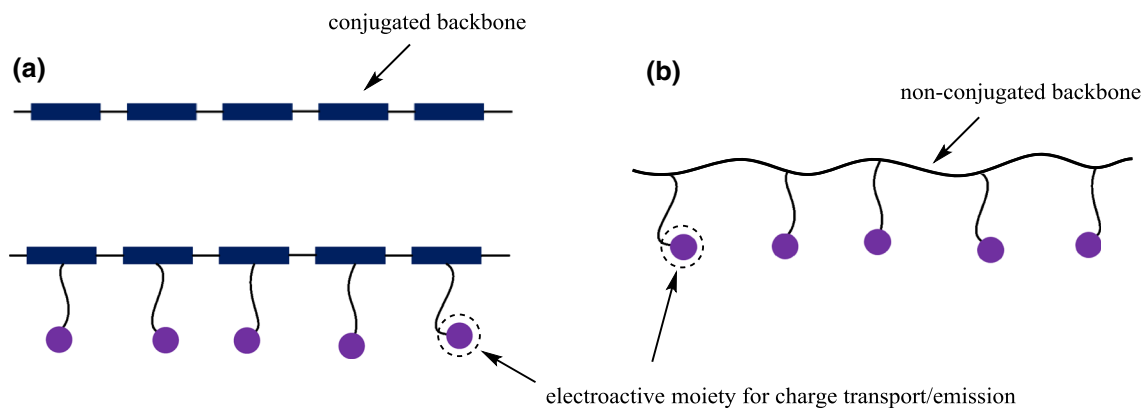
Fig. 2. Polymer with conjugated backbone, which by itself fulfils the purpose of charge transport and/or emission (a, top). Polymer with conjugated backbone with pendent electroactive moieties for additional desired properties (a, bottom). Polymer with non-conjugated backbone with pendent electroactive moieties for charge transport and/or emission (b).
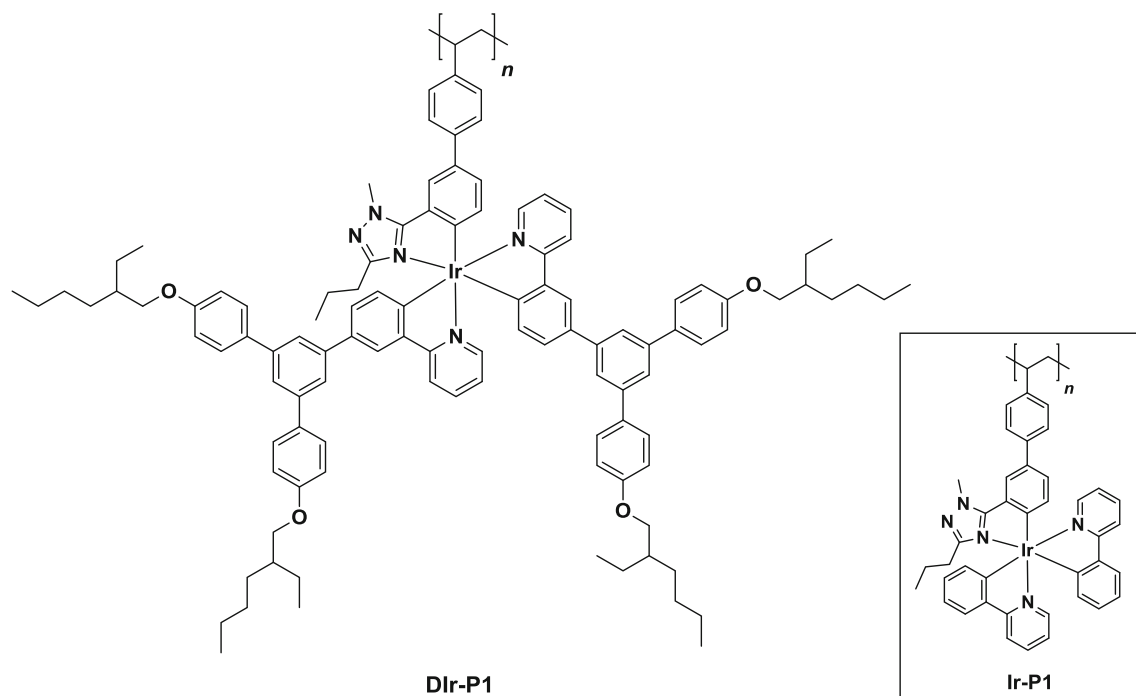

Fig. 3. Polystyrene containing pendant iridium(III) phosphor (**DIr-P1**) functionalized with bulky 1,3-bis(2-ethylhexyloxyphenyl)phenyl dendrons to suppress interchromophore interactions. Also shown in the inset is the non-dendronized reference polymer (**Ir-P1**).

former. **DIr-P1** showed a green emission with λ_{PL} (emission maximum of photoluminescence) at 518 nm with a shoulder at 548 nm in degassed DCM, and its neat film emission spectrum was essentially identical. The device [ITO/20 wt.% **DIr-P1** in CBP/TPBI (60 nm)/LiF (0.7 nm)/Al (>100 nm)] (see Table SII for the chemical nomenclature and structures of OLED materials mentioned in this review) gave a green λ_{EL} (emission maximum of electroluminescence) at 520 nm with CIE at (0.34, 0.62). The maximum EQE of 7.5% was attained, when device emission became detectable, and the efficiency roll-off was small so that the EQE

dropped slightly to 6.2% and 5.5% at luminance of 100 and 1000 cd m^{-2}, respectively.

Levell and coworkers also reported a similar dendronized phosphorescent iridium(III) polymer (**DIr-P2**, Fig. 4) which had a 2-(2-pyridyl)-1,3,4-triazole ligand and a norbornenyl polymer backbone instead of the 2-phenyl-1,3,4-triazole ligand and a polystyrene backbone in **DIr-P1**.[27] **DIr-P2** showed a green emission with λ_{PL} at 497 nm and a shoulder at 525 nm in degassed DCM. Its Φ_{PL} of 37% was slightly lower than that of the reference compound (**DIr-M2**, Φ_{PL}: 53%), suggesting the presence of interchromophore interactions in the polymer due
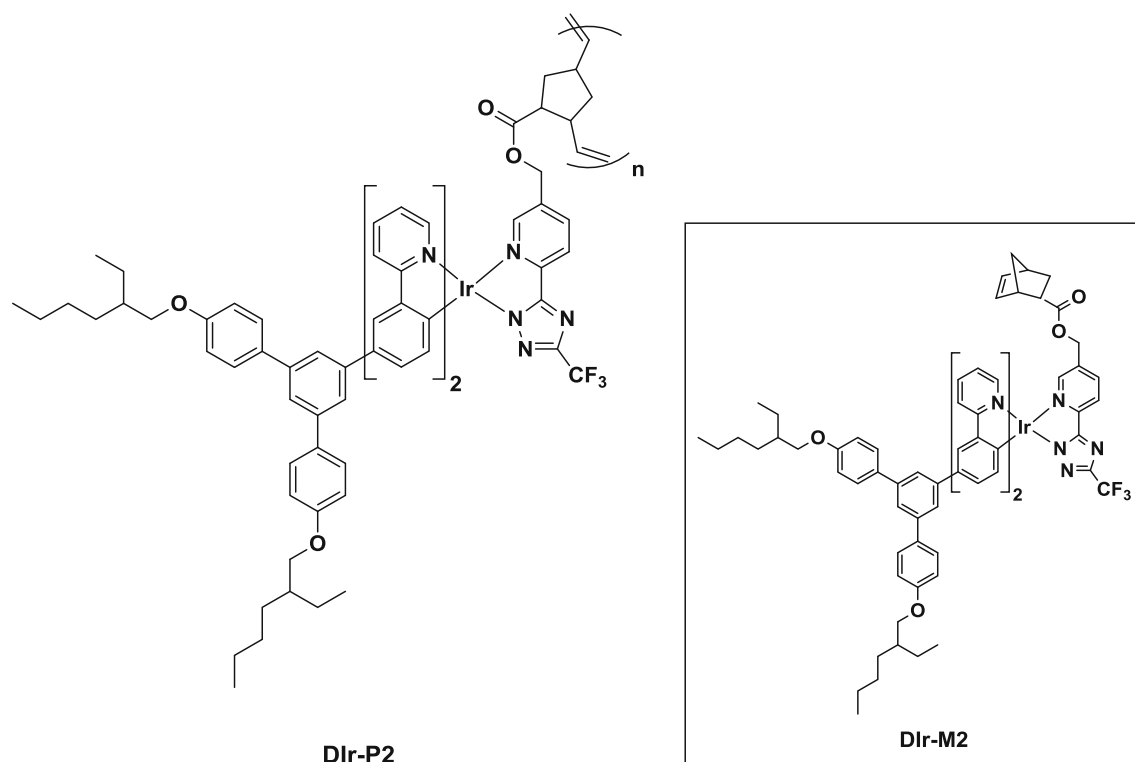
Fig. 4. Dendronized phosphorescent iridium(III) polymer (**DIr-P2**) based on norbornenyl backbone. Also shown in the inset is the monomer (**DIr-M2**) as the reference emitter.

to the close proximity of iridium(III) phosphors along the polymer chain. Both **DIr-P2** and **DIr-M2** neat films exhibited emissions slightly red-shifted by *ca.* 5–10 nm compared with those in DCM and their Φ_{PL} values were significantly lowered to 15% and 13%, respectively. Yet, the Φ_{PL} of neat **DIr-P2** (15%) was much better than that of the non-dendronized analogue (<1%) reported previously,[28] thus proving the effectiveness of the dendrons. Given that **DIr-P2** doped in CBP (20 wt.%) showed a much improved Φ_{PL} of 52% than the polymer neat film, it was employed as the emitting layer in the PLED device [ITO/20 wt.% **DIr-P2** in CBP (~100 nm)/TPBI (60 nm)/LiF (0.7 nm)/Al (100 nm)] which gave an EQE and a current efficiency of 5.1% and 16.4 cd A^{-1}, respectively, at a brightness of 100 cd m^{-2} under an applied voltage of 15.8 V. The emission was green with CIE coordinates at (0.32, 0.60).

Given that the aforementioned homopolymers **DIr-P1** and **DIr-P2** could not suppress interchromophore interactions completely, even though they were dendronized, Levell et al. then developed a copolymerization strategy as a resolution.[29] They prepared a random copolymer (**DIr-P1-*co*-S**, Fig. 5) between **DIr-P1** and polystyrene by free-radical copolymerization. According to nuclear magnetic resonance (NMR) integration, the molar ratio of styrene units to the dendronized iridium(III) chromophores was found to be 75:1. In DCM solution, **DIr-P1-*co*-S** had the same emission spectrum as

DIr-P1 with λ_{PL} at 517 nm, which suggested that the styrene units did not take part in the photophysical processes. In addition, **DIr-P1-*co*-S** had an excellent Φ_{PL} of 94%, which was comparable to that of the reference emitter (**DIr-M3**, Φ_{PL}: 92%) whereas the Φ_{PL} of the homopolymer **DIr-P1** was significantly lower (61%).[26] Furthermore, the doped film of **DIr-P1-*co*-S** (20 wt.% in CBP) showed a much improved Φ_{PL} of 67% compared with the **DIr-P1** case (Φ_{PL}: 42%). All these results proved that the copolymerization strategy succeeded in completely suppressing interchromophore interactions thanks to the styrene units as spacer. Despite the enhanced photophysical properties of the copolymer, device [ITO/20 wt.% **DIr-P1-*co*-S** in CBP (~100 nm)/TPBI (60 nm)/LiF (0.7 nm)/Al (>100 nm)] offered an EQE of 6.7% at a luminance of 100 cd m^{-2} which was only comparable to that of the homopolymer **DIr-P1** device (EQE: 6.2%). Indeed, while styrene units in the copolymer were fully functional in diluting the phosphors, they were not electroactive, and; hence, the hole mobility of the copolymer suffered, followed by limited device performance.

Levell et al. then reported a follow-up study by replacing insulating styrene units with electroactive carbazole functionality to boost the hole mobility of the polymers,[30] given poly(*N*-vinylcarbazole) is a widely employed hole-transporting material.[11] They prepared a series of random copolymers (**Ir-P1-*co*-VK**, **DIr-P1-*co*-VK** and **DDIr-P1-*co*-VK**, Fig. 6)

Recent Advances in Polymer Organic Light-Emitting Diodes (PLED) Using Non-conjugated
Polymers as the Emitting Layer and Contrasting Them with Conjugated Counterparts

6251
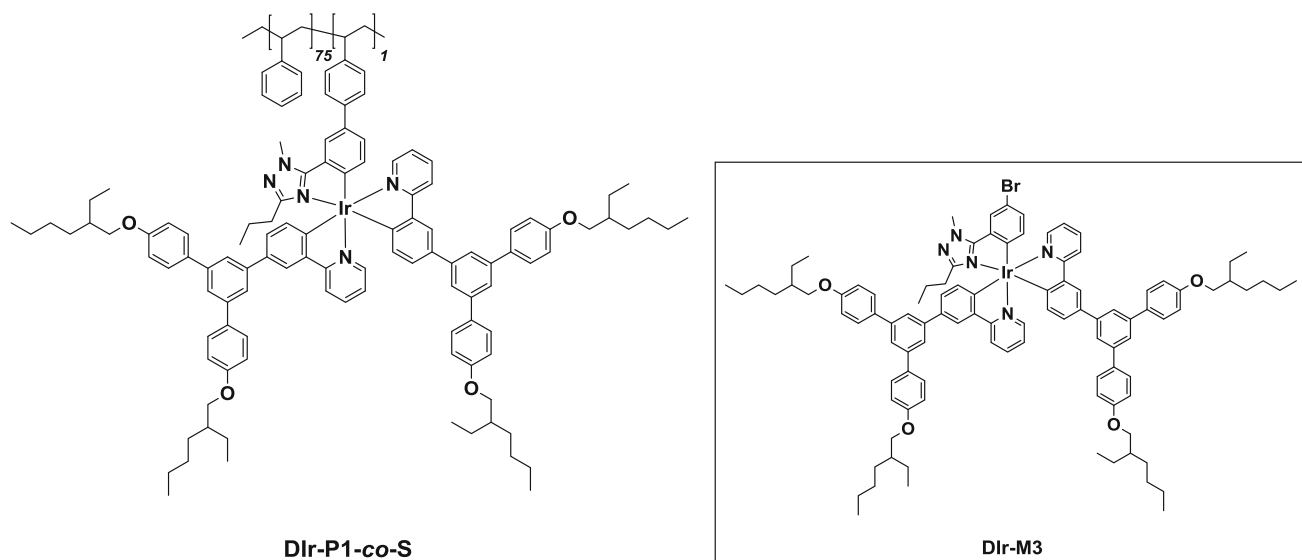

DIr-P1-*co*-S

DIr-M3

Fig. 5. A copolymer (**DIr-P1-*co*-S**) between polystyrene and **DIr-P1** where the styrene units acted as spacer to prevent undesirable interchromophore interactions. Also shown in the inset is the reference emitter (**DIr-M3**).
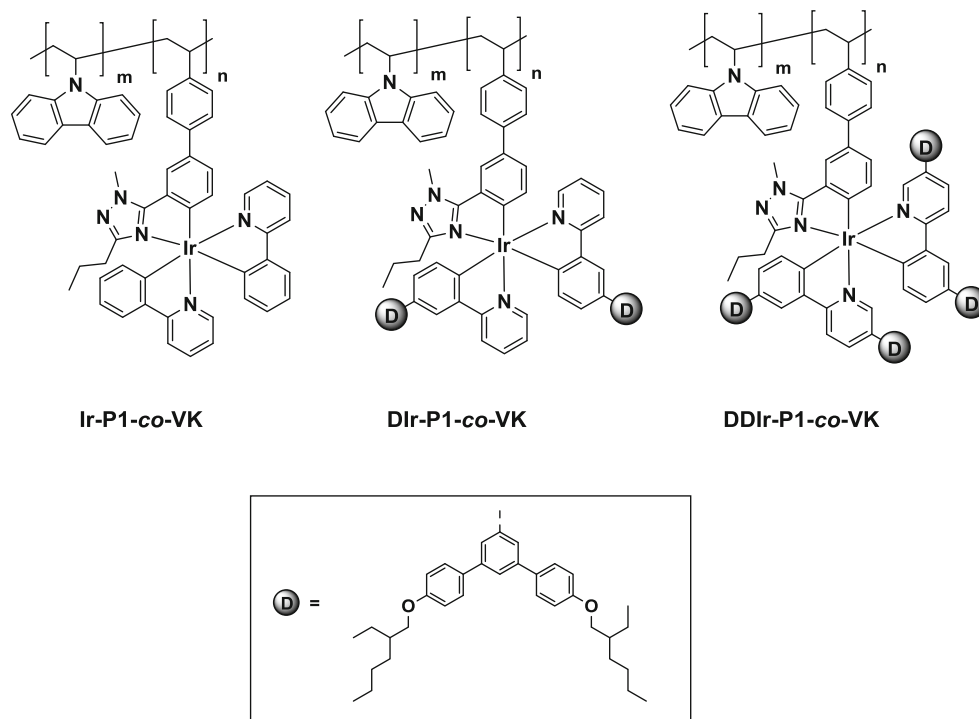

Ir-P1-*co*-VK **DIr-P1-*co*-VK** **DDIr-P1-*co*-VK**

D =

Fig. 6. Three copolymers between poly(*N*-vinylcarbazole) and polystyrene with pendant iridium(III) phosphors having none (**Ir-P1-*co*-VK**), one (**DIr-P1-*co*-VK**) and two (**DDIr-P1-*co*-VK**) dendrons on each ligand. Also shown in the inset is the 1,3-bis(2-ethylhexyloxyphenyl)phenyl dendron.

with carbazole to phosphor monomer feed ratios of 55–72 to 1, but the authors could not obtain the monomer compositions in the resulting copolymers due to the broadness and significant overlap of NMR signals. In DCM solutions, **Ir-P1-*co*-VK**, **DIr-P1-*co*-VK** and **DDIr-P1-*co*-VK** showed green λ_{PL} at 512 nm, 516 nm and 551 nm, respectively, which were basically identical to those of the homopolymers (**Ir-P1**, **DIr-P1** and **DDIr-P1**, Fig. 7, *vide infra*),[31] implying efficient energy transfer from carbazole moieties to the phosphors. Their Φ_{PL} values were found to be 69%, 64%, and 64%, respectively, which were lower than **DIr-P1-*co*-S** (Φ_{PL}: 94%)[29] due to back triplet energy transfer from the phosphors to the carbazole units (poly(*N*-vinylcarbazole) has a low triplet energy of 2.5 eV).
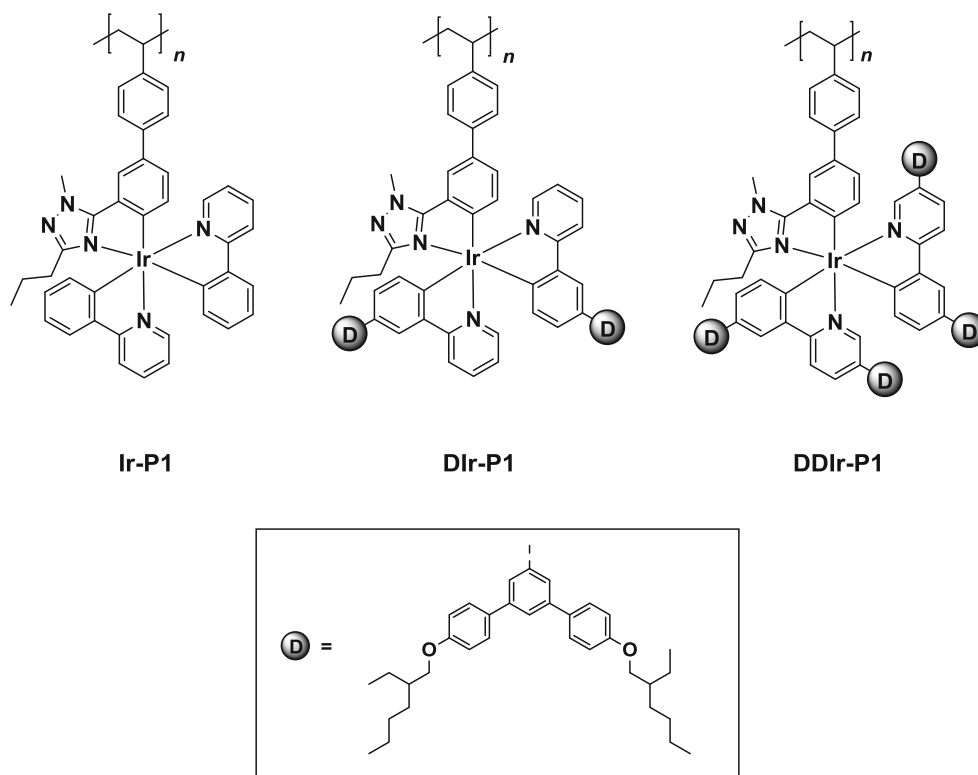
Fig. 7. Polystyrenes with pendant iridium(III) phosphors having none (**Ir-P1**), one (**DIr-P1**) and two (**DDIr-P1**) dendrons on each ligand. Also shown in the inset is the 1,3-bis(2-ethylhexyloxyphenyl)phenyl dendron.

The device [ITO/50 wt.% **DDIr-P1-*co*-VK** in CBP (*ca.* 100 nm)/TPBI (60 nm)/LiF (0.7 nm)/Al (>100 nm)] gave the best EQE of 14.7% at 100 cd m^{-2}. Devices with the same architecture, while using neat **Ir-P1-*co*-VK**, **DIr-P1-*co*-VK** and **DDIr-P1-*co*-VK** as the emitting layers, were also fabricated, but lower EQEs (10.0–11.0%) were obtained. Given that Φ_{PL} of neat films of the copolymers (46–57%) were considerably lower than that of 50 wt.% **DDIr-P1-*co*-VK** doped in CBP film (Φ_{PL}: 73%), it was concluded that the efficiencies of these devices were determined by the Φ_{PL} values of the emitting layers.

In addition to copolymerization strategy, Lai and co-workers proposed a "double-dendron" approach to solve the interchromophore interaction problem.[31] They contrasted three polymers **Ir-P1**, **DIr-P1** and **DDIr-P1** (Fig. 7) to investigate how the number of dendrons on the central iridium(III) phosphor impacted the photophysical properties and device performances of the polymers. In the DCM solution, Φ_{PL} of **Ir-P1**, **DIr-P1** and **DDIr-P1** were 23%, 61%, and 67%, respectively, while their neat films all showed diminished Φ_{PL} of <1%,[26] 13%, and 47%, respectively. These results demonstrated a clear trend that increasing the number of dendrons on the phosphor effectively suppressed interchromophore interactions in the polymers. It is worth noting that while **Ir-P1** and **DIr-P1** had very similar emission energies (**DIr-P1** λ_{PL}: 518 nm), the

λ_{PL} of **DDIr-P1** was significantly red-shifted by *ca.* 30 nm to 551 nm, as a result of effective conjugation length increase in the ligands. A PLED device [ITO/ **DDIr-P1** (75 nm)/TPBI (60 nm)/LiF (0.7 nm)/Al (>100 nm)] gave a yellow emission with CIE at (0.48, 0.51). An EQE of 9.2% was achieved at 100 cd m^{-2} with a low efficiency roll-off so that the EQE dropped slightly to 8.4% at 1000 cd m^{-2}. On the other hand, a device with same structure based on **DIr-P1** gave a lower EQE of 6.2% at 100 cd m^{-2} even though the polymer was doped in CBP host (20 wt.%), hence, proving the effectiveness of the dendrons.

Lai and co-workers also synthesized a series of similar polymers (**Ir-P3**, **DIr-P3** and **DDIr-P3**, Fig. 8) whose backbone was derived from norbornene using ring-opening metathesis polymerization (ROMP).[32] The key merit of these polymers was their narrower polydispersity index (PDI) of *ca.* 1.4 than those with polystyrene backbone (**Ir-P1**, **DIr-P1** and **DDIr-P1**)[31] prepared by free-radical copolymerization (e.g., **DDIr-P1** had a PDI as high as 4). PLED performances based on conjugated polymers have been found to depend on their PDIs.[33,34] In line with the results obtained from polystyrene analogues (**Ir-P1**, **DIr-P1** and **DDIr-P1**),[31] it has been shown a clear positive correlation between the number of dendrons on the ligands and the Φ_{PL} of the polymers both in solution and neat films. For example, Φ_{PL} of **Ir-P3**, **DIr-P3** and **DDIr-P3** in

Recent Advances in Polymer Organic Light-Emitting Diodes (PLED) Using Non-conjugated
Polymers as the Emitting Layer and Contrasting Them with Conjugated Counterparts

6253
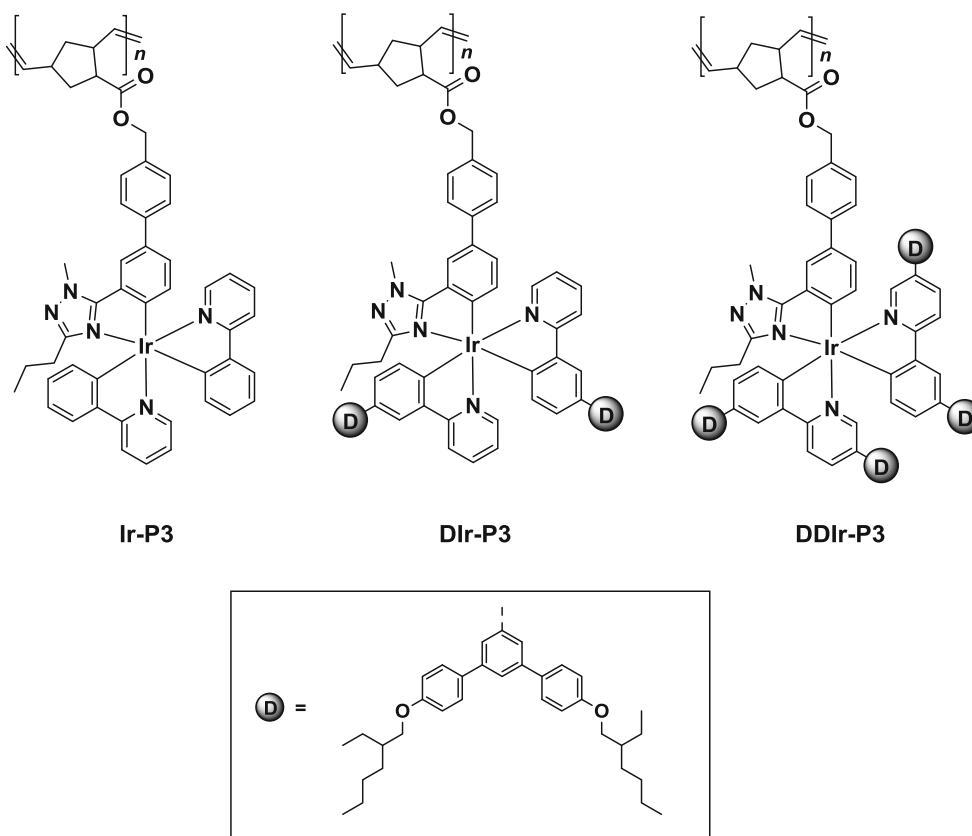
Ir-P3   **DIr-P3**   **DDIr-P3**

D =

Fig. 8. Polymers with norbornene-derived backbone by ring-opening metathesis polymerization (ROMP) with pendant iridium(III) phosphors having none (**Ir-P3**), one (**DIr-P3**) and two (**DDIr-P3**) dendrons on each ligand. Also shown in the inset is the 1,3-bis(2-ethylhexyloxyphenyl)phenyl dendron.
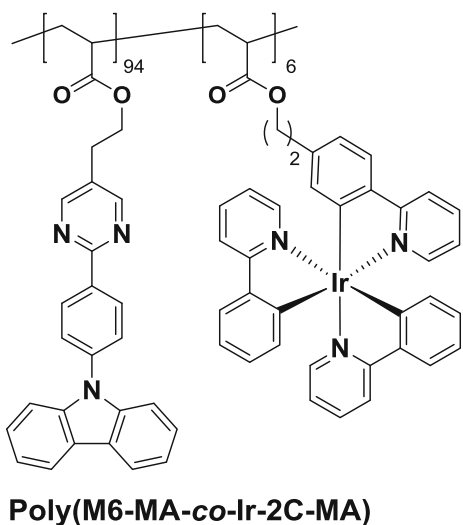

Poly(M6-MA-*co*-Ir-2C-MA)

Fig. 9. A random copolymer (**Poly(M6-MA-*co*-Ir-2C-MA)**) between carbazole-pyrimidine based host and pendant Ir(ppy)$_3$ phosphor with a methyl methacrylate backbone for single-layer PLED applications.

DCM solutions were 48%, 65%, and 71%, respectively. In neat films, their values were lowered to 2,% 44%, and 58%, respectively. However, no PLED devices were fabricated in this study.

Page et al. very recently reported a library of random copolymers consisting of a carbazole-pyrimidine bipolar host and a pendant Ir(ppy)$_3$ phosphor for PLED applications (the best performing copolymer among the series, **Poly(M6-MA-*co*-Ir-2C-MA)**, is shown in Fig. 9).[35] They found that the PLQYs of the polymer neat films decreased with increasing Ir(ppy)$_3$ phosphor concentrations (0.5–29 mol.%), suggesting the presence of undesirable interchromophore interactions in the film when the phosphor content became more concentrated, which is consistent with the observations reported in the aforementioned studies.[27,29,31] Although the copolymer with 0.5 mol.% Ir(ppy)$_3$ phosphor exhibited the best PLQY of 81% among the series, a minimum of 3 mol.% phosphor was required to complete the energy transfer from the host to the dopant. Thanks to the bipolar characteristics of the host to facilitate both hole and electron injections and transport, a single-layered PLED [ITO/AQ1200/**Poly(M6-MA-*co*-Ir-2C-MA)** (∼30 nm)/LiQ (2 nm)/Al (100 nm)] was fabricated, where a 6 mol.% phosphor was found to show the best compromise between PLQY and charge transport in the polymeric emitting layer. The device gave a green emission (λ_{EL}: ∼520 nm) with a maximum current efficiency of 3.6 cd A^{-1}.
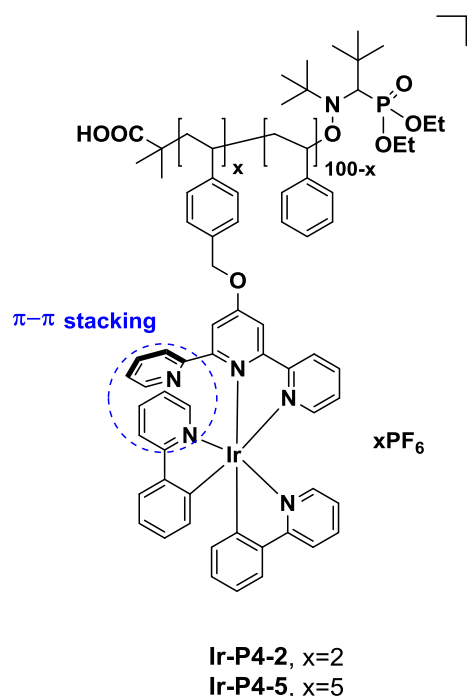
Fig. 10. Two random copolymers of styrene and a cationic iridium(III) phosphor with PF_6^- as the counter anion (**Ir-P4-2** and **Ir-P4-5**). The π-π stacking between the non-coordinating pyridine moiety of the terpyridine ligand and the pyridine ring of adjacent phenylpyridine ligand is highlighted in blue, which results in enhanced emitter stability.

Dumur and co-workers reported a series of two random copolymers of styrene and a cationic iridium(III) phosphor with PF_6^- as the counter anion (**Ir-P4-2** and **Ir-P4-5**, Fig. 10, which contained 2 mol.% and 5 mol.% of phosphor, respectively).[36] A distinct feature of the pendant iridium(III) complex was the strong π-π stacking between the non-coordinating pyridine moiety of the terpyridine ligand and the pyridine ring of adjacent phenylpyridine ligand, hence, creating a steric bulk around the complex to decrease its accessibility to nucleophilic quenchers and increase its stability.[37] Being ionic, **Ir-P4-2** and **Ir-P4-5** had the potential for light-emitting electrochemical cell (LEEC) applications. LEEC is an alternative to OLED as a light-emitting device, which enjoys a simpler device architecture and fabrication procedure, because it is usually single-layered and has the ionic emitting layer spun-coated on the anode substrate.[38–41] Furthermore, air-stable cathodes (e.g., Al[40] and Ag[41]) can be employed for LEEC devices to reduce device encapsulation cost. **Ir-P4-2** and **Ir-P4-5** were synthesized by nitroxide mediated polymerization (NMP) so that they had low PDIs of 1.16 and 1.17, respectively. **Ir-P4-2** and **Ir-P4-5** neat films gave green λ_{PL} at 539 nm and 553 nm, respectively, suggesting more prominent chromophore aggregation in the latter due to its higher phosphor concentration. Blend films of **Ir-P4-2** and **Ir-P4-5**

with poly(*N*-vinylcarbazole) (w/w = 1:1) resulted in slightly blue-shifted λ_{PL} at 526 nm and 532 nm, respectively. However, no Φ_{PL} data were reported. It was found that only **Ir-P4-5** was able to function in light-emitting devices, whereas **Ir-P4-2** failed to give any emissions because the concentration of insulating styrene units was too large for efficient charge hopping in the polymer. LEEC device [ITO/PEDOT:PSS (40 nm)/PVK/**Ir-P4-5**/Ca (300 nm)] offered a luminance of 70 cd m^{-2} under high voltage of 24 V. On the other hand, an OLED device [ITO/PEDOT:PSS (40 nm)/50 wt.% **Ir-P4-5** blend with PVK/Ca (300 nm)] gave a poor luminance of 5 cd m^{-2} at 30 V.

Shao and co-workers prepared a series of polymer (**Ir-P5-x**, Fig. 11) based on a fluorinated poly(arylene ether phosphine oxide) backbone with varying concentrations of pendant yellow phosphor (fbi)$_2$Ir(-acac) (1–4 mol.%).[42] The key merit of the polymer backbone is its bipolar characteristics with the highest occupied molecular orbital (HOMO) and the lowest unoccupied molecular orbital (LUMO) levels at −5.7 eV and −2.3 eV, respectively, due to the presence of carbazole donor and triphenylphosphine oxide acceptor moieties, yet maintaining a high triplet energy (E_T) of 2.96 eV. The authors attributed the high triplet energy to the electronic isolation effect of the oxygen atoms. A series of polymers were prepared with varying compositions of (fbi)$_2$Ir(acac) (1–4 mol.%). In photoluminescence measurements, it was found that a minimum concentration of 4 wt.% (fbi)$_2$Ir(acac) in the polymer was required to attain almost complete Forster energy transfer from the host to the phosphor. However, a lower amount of 2 wt.% of (fbi)$_2$Ir(acac) was required in electroluminescence to achieve this due to charge trapping by the yellow phosphor, given its shallower HOMO level (−5.1 eV) and deeper LUMO level (−2.7 eV) than those of the host. The best PLED device [ITO/PEDOT:PSS (40 nm)/**Ir-P5-0.03** (40 nm)/TPCz (50 nm)/LiF (1 nm)/Al (100 nm)] offered λ_{EL} at 566 nm and CIE at (0.53, 0.46) with an EQE of 4.1% and a current efficiency of 10.4 cd A^{-1}. The group also simultaneously reported an identical polymer system with pendant blue phosphor (FIrpic) whose device [ITO/PEDOT:PSS (40 nm)/**polymer** (40 nm)/TPCz (50 nm)/LiF (1 nm)/Al (100 nm)] achieved a decent EQE of 9.0%.[43]

The group then extended the work by combining the blue and yellow phosphors to prepare a bichromophoic polymer for white PLED applications (**Ir-P5-x-y**, Fig. 12). By carefully tuning the relative compositions of the blue (**x** mol.%) and yellow (**y** mol.%) phosphors, white emission could be obtained.[44] The high triplet energy of the host (2.96 eV) was particularly important to prevent back energy transfer from the blue phosphors (E_T: 2.65 eV). The best white PLED [ITO/PEDOT:PSS (40 nm)/**Ir-P5-0.075-0.007** (40 nm)/TPCz (50 nm)/LiF (1 nm)/Al (100 nm)] attained an EQE and a

Recent Advances in Polymer Organic Light-Emitting Diodes (PLED) Using Non-conjugated
Polymers as the Emitting Layer and Contrasting Them with Conjugated Counterparts
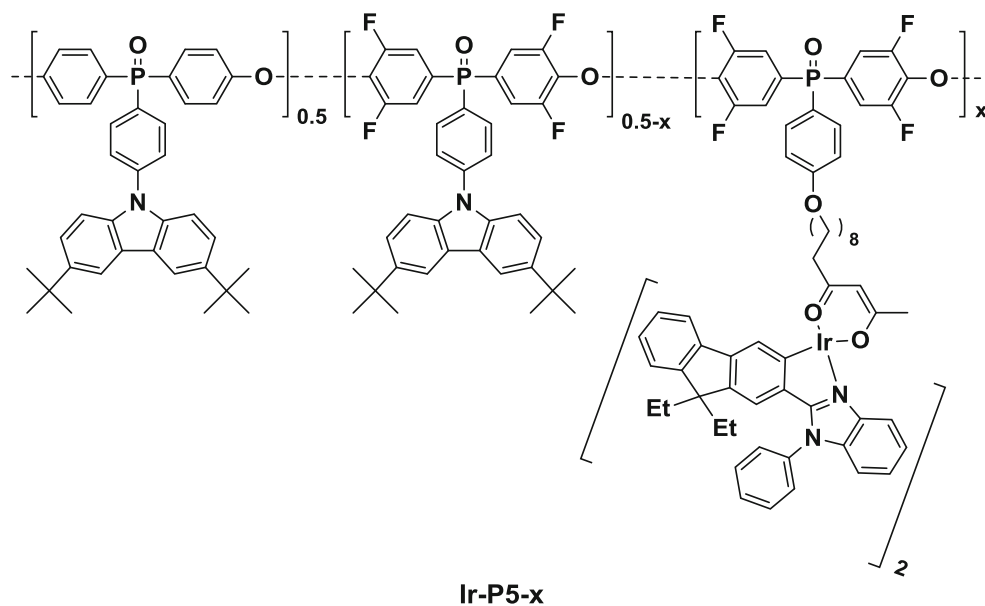
6255

Ir-P5-x

Fig. 11. A polymer based on a fluorinated poly(arylene ether phosphine oxide) backbone with varying concentrations of pendant yellow phosphor (**Ir-P5-x**, **x**: 0.01–0.04).
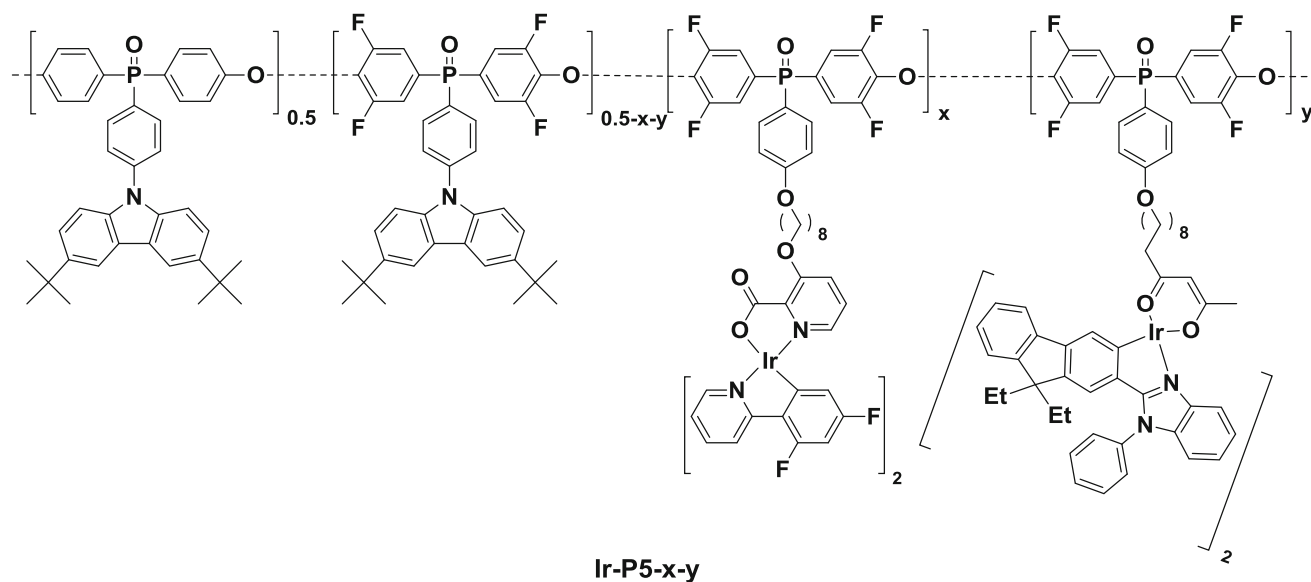

Ir-P5-x-y

Fig. 12. A bichromophoic polymer (**Ir-P5-x-y**) containing **x** mol.% and **y** mol.% of blue and yellow phosphors for white PLED applications.

current efficiency of 7.1% and 18.4 cd A^{-1}, respectively, with CIE at (0.31, 0.43).

Park and co-workers developed a series of blue (**Ir-P6(mCP-*co*-B)**), green (**Ir-P6(CBP-*co*-G)**) and red (**Ir-P6(CBP-*co*-R)**) phosphorescent copolymers for PLED applications (Fig. 13).[45] The copolymers consisted mainly of host with a small amount of respective phosphors [mCP for blue FIracac; CBP for both green (ppy)$_2$Ir(acac) and red (btp)$_2$Ir(acac)]. Phosphor compositions: 1.7–13.9 mol.%. Vinyl addition polymerization of norbornene-functionalized monomers using Pd(II) catalysis produced high molecular weight polymers (M_w: 151–457 kDa).

The copolymers demonstrated excellent thermal stabilities (T_gs > 330°C). In solutions, all the copolymers showed both high-energy emissions (*ca*. 350–400 nm) from the hosts and low-energy emissions from the phosphors. However, the emission spectra of the copolymer neat films were mainly contributed by the phosphors. These results indicated that energy transfer from host to the phosphor was much more efficient in neat film compared with that in solutions. All the copolymers were tested for PLED performances with the device structure: ITO/PEDOT:PSS (40 nm)/**copolymer**/(40 nm)/TPBI (15 nm)/Bphen (35 nm)/LiF (1 nm)/Al (100 nm). The
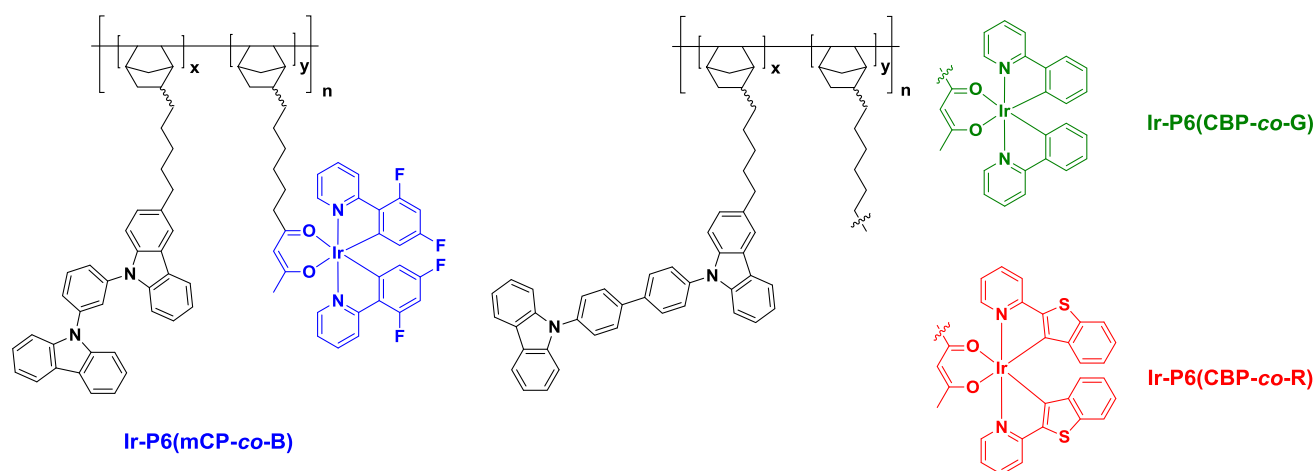
Fig. 13. Three series of blue (**Ir-P6(mCP-*co*-B)**), green (**Ir-P6(CBP-*co*-G)**) and red (**Ir-P6(CBP-*co*-R)**) phosphorescent copolymers of host monomers and respective phosphors.
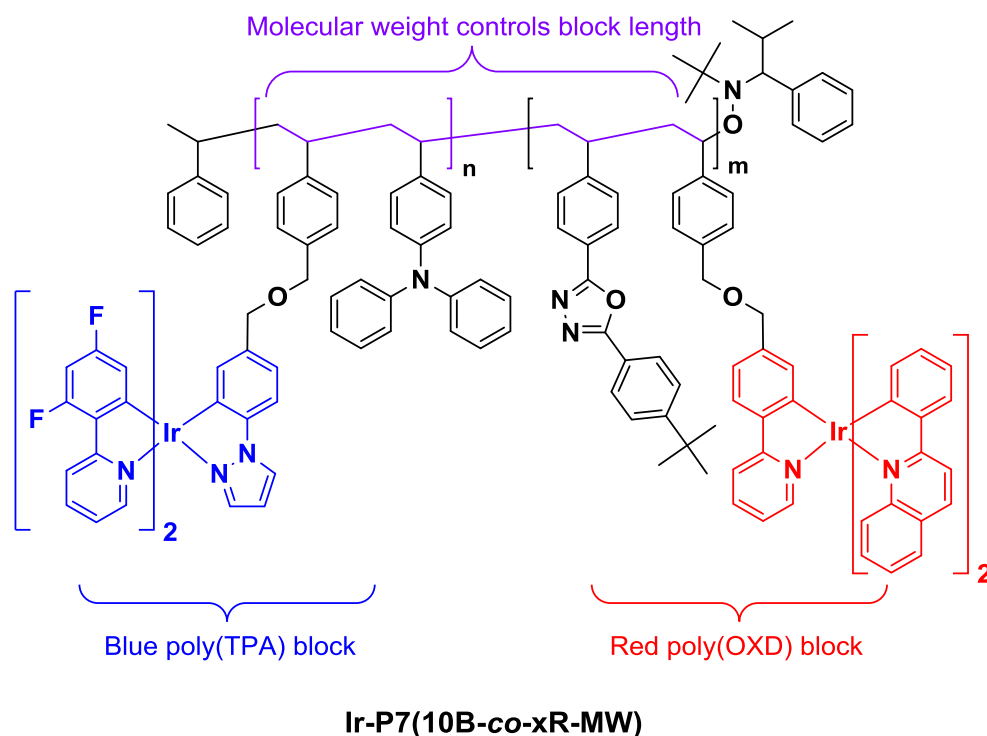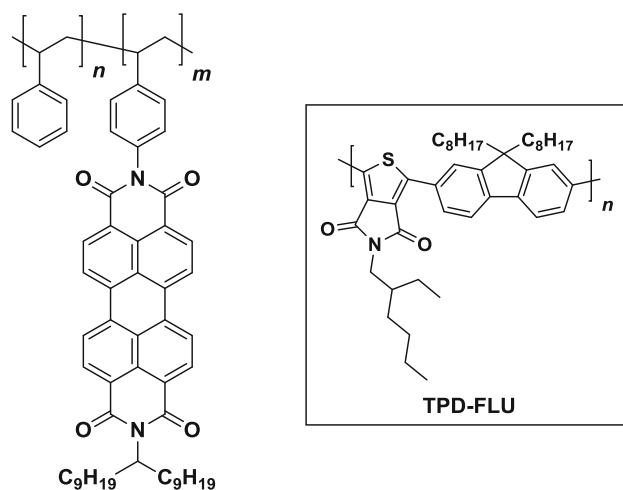

Ir-P7(10B-*co*-xR-MW)

Fig. 14. A biphasic white-emitting block copolymer, **Ir-P7(10B-*co*-xR-MW)**, consisting of poly(TPA) copolymerized with blue phosphor (always 10 wt.%) and poly(OXD) with varying amount of red phosphors (x = 0.1–2 wt.%). The molecular weight of the polymer is the key factor for successful site isolation.

best blue device was offered by the polymer with 10.5 mol.% phosphor, which gave λ_{EL} at 488 nm with an EQE of 8.8%. On the other hand, the best green and red devices were fabricated with polymers with 5.3 mol.% and 13.9 mol.% phosphors, respectively, which showed λ_{EL} at 522 nm and 619 nm with EQEs of 13.3% and 5.1%, respectively.

Poulsen et al. employed a strategy of biphasic block copolymer (**Ir-P7(10B-*co*-xR-MW)**, Fig. 14) to achieve site isolation in which energy transfer from the high-energy phosphor to the low-energy one

could be controlled so that white emission could be generated.[46] The first block consisted of poly(TPA) randomly copolymerized with a small amount of blue phosphor (10 wt.%) while the second block contained poly(OXD) randomly copolymerized with an even smaller amount of red phosphor (0.1–2 wt.%). The two blocks were always of the same length to allow systematic study of how block length impacted the morphological properties of the polymer. It was found that the molecular weight of the polymer (i.e., block length) was critical to the

Recent Advances in Polymer Organic Light-Emitting Diodes (PLED) Using Non-conjugated
Polymers as the Emitting Layer and Contrasting Them with Conjugated Counterparts

6257

PS-PERY-8: *n/m*=24
PS-PERY-16: *n/m*=76

Fig. 15. Two copolymers of styrene and a red-emitting PDI chromophore, **PS-PERY-8** and **PS-PERY-16** with 4 mol.% and 1.3 mol.% of PDI units in a polymer chain, respectively. Also shown in the inset is a green-emitting polymer **TPD-FLU**.

success of site isolation. For example, a copolymer with a low number average molecular weight (M_n) of 30 kDa did not show any phase separation under the examination of transmission electron microscopy (TEM). However, copolymers with higher M_n from 100 kDa to 150 kDa demonstrated well-separated domains with clear nano-sized lamellar morphology. A single-layer white PLED [ITO/**Ir-P7(10B-*co*-1R-100)**/LiF (1 nm)/Al (100 nm)] using a copolymer of 100 kDa molecular weight with blue to red phosphor ratio of 10% to 1% gave the best EQE of 1.5%. Consistent with the TEM results, for a given ratio of blue to red phosphor (10% to 1% or 10% to 0.5%), the contribution of red emission fell when the molecular weight of the polymers increased. Yet, no CIE coordinates of the emissions were reported.

From the phosphorescent polymers discussed, it can be observed that both dendrimer and copolymerization approaches managed to reduce interchromophore interactions along the polymer chain to improve the photophysical properties of the polymers, and a combined use of these two strategies helped to create the optimal device. For example, the highest EQE obtained by **DDIr-P1-*co*-VK** copolymer was 14.7%,[30] nearly 50% higher than that of **DDIr-P1** homopolymer (EQE: 9.2%).[31] One likely reason is that the 1,3-bis(2-ethylhexyloxyphenyl)phenyl dendron was neither a *p*-type nor a *n*-type moiety, and; hence, charge transport in the emitting layer was hampered. A similar phenomenon has been observed in **DIr-P1-*co*-S** in which the insulating styrene units limited the device efficiency as a result of compromised charge mobility.[29] Two strategies for white PLED have

been discussed: biphasic **Ir-P7(10B-*co*-xR-MW)** for chromophore isolation[46] and concentration control of the high-energy and low-energy phosphors in (**Ir-P5-x-y**) for mutual emission.[44] The achieved EQEs were 1.5% and 7.1%, respectively. Another strategy for site isolation is to employ dendritic structure in the polymer[47,48] which is worth a future research effort.

Fluorescent Polymers

Fluorescent emitters are typically made of light elements (C, H, O, N, etc.), and; therefore, the vast majority of them are organic materials. Unlike phosphorescent organometallic complexes, most fluorescent emitters have very slow intersystem-crossing (ISC) rates, and; hence, only the singlet excitons can emit. As a result, the maximum IQE achievable is 25%. Assuming lambertian emission, which results in an outcoupling efficiency of about 20%, the maximum EQE of fluorescence devices will be $25\% \times 20\% = 5\%$.[49] However, the main advantage of fluorescent emitters over phosphorescent counterparts is the employment of economical organic materials instead of expensive rare metal complexes.

Perylene diimide is an ideal red chromophore with excellent quantum efficiency in dilute solution and supreme photochemical stability.[50] However, due to its largely planar structure, intermolecular face-to-face stacking results in severe aggregation-caused quenching (ACQ).[51] Therefore, Kozma et al. prepared two random copolymers of styrene and a red perylene diimide chromophore (**PS-PERY-8** and **PS-PERY-16**, Fig. 15) by nitroxide mediated radical polymerization (NMP) in which the styrene units acted as an inter-chromophore spacer.[51] **PS-PERY-8** and **PS-PERY-16** contained 4 mol.% and 1.3 mol.% of perylene diimide units respectively in a polymer chain. Both copolymer neat films showed a broad emission from 500 nm to 700 nm, but **PS-PERY-16** exhibited a better Φ_{PL} of 83% than **PS-PERY-8** (Φ_{PL}: 68%) which can be explained by more effective suppression of aggregation-caused quenching (ACQ) in **PS-PERY-16** due to its higher styrene content. This was further evidenced by the much lower Φ_{PL} of 23% when polystyrene film was blended with the corresponding amount (4 mol.% or 1.3 mol.%) of perylene diimide vinyl monomer. Instead of a PLED device, a hybrid one was fabricated, where a commercial blue light-emitting diode (Osram) was employed to provide blue light and to act as the excitation light source for a known green polymer (**TPD-FLU**), and the aforementioned red polymer **PS-PERY-16**, resulting in a white light device with an EQE and power efficiency of 5% and 28 lm W^{-1}, respectively. The CIE coordinates were (0.31, 0.34) and the color-rendering index (CRI) was 83.

Wang and Leung reported two novel blue fluorescent polymers **P(2ADN)** and **P(3ADQ)**[52] where the
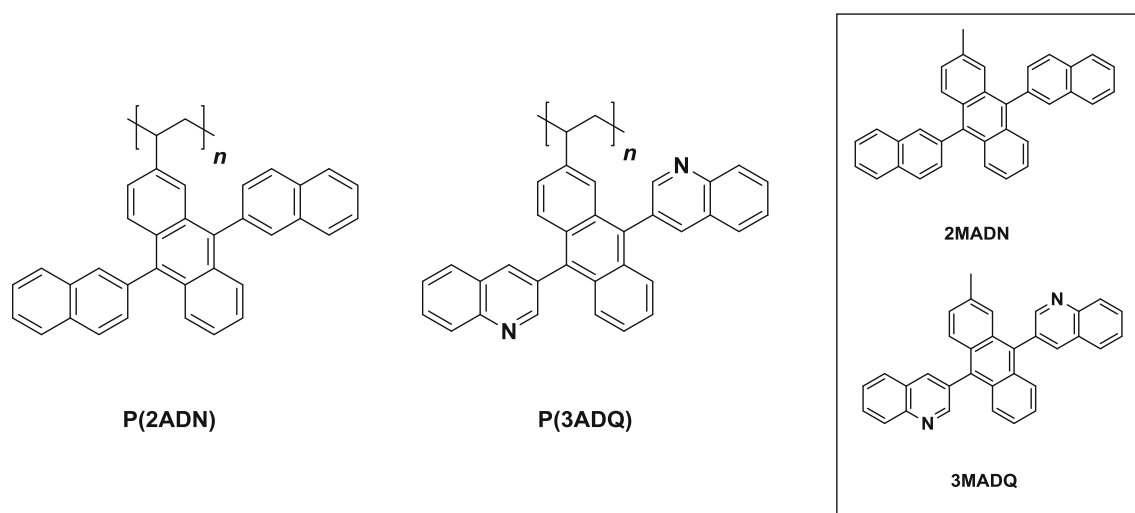
Fig. 16. Blue fluorescent polymers **P(2ADN)** and **P(3ADQ).** Also shown in the inset are their reference compounds, **2MADN** and **3MADQ**.
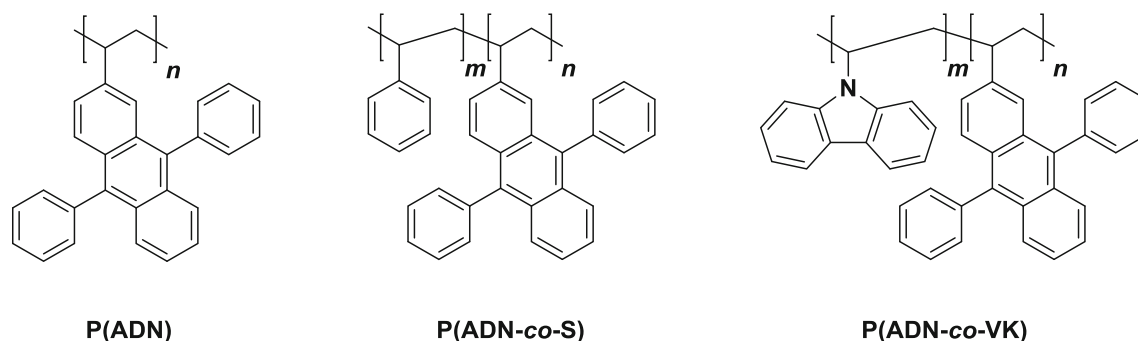

Fig. 17. The deep-blue homopolymer of 9,10-di(2-naphthalenyl)anthracene, **P(ADN)**, and its random copolymers with styrene, **P(ADN-*co*-S)**, and carbazole, **P(ADN-*co*-VK)**.

former was derived from the well-noted blue emitter **2MADN**[53] (Fig. 16). **P(2ADN)** and **P(3ADQ)** exhibited very high glass-transition temperatures (T_gs) of 343°C and 298°C, respectively. Interestingly, **P(3ADQ)** could be dissolved in ethanol/water mixture ($v:v$ = 1:1) despite its high composition of hydrophobic aromatic rings and alkyl side chain, which was likely the result of extensive hydrogen-bonding between the pyridine-type nitrogen atoms and the protic solvents. **P(2ADN)** and **P(3ADQ)** showed λ_{PL} at 443 nm and 452 nm in THF, respectively, both slightly red-shifted compared with their reference compounds (**2MADN**: λ_{PL} at 426 nm and **3MADQ**: λ_{PL} at 436 nm) which was attributed to the enhanced aggregation of chromophore brought into close proximity by the polymer side chains. In addition, **P(2ADN)** and **P(3ADQ)** exhibited significantly lower Φ_{PL} of 43% and 24%, respectively, than their reference compounds (80% and 41%, respectively), further suggesting the presence of chromophore aggregation in the polymer. Neat films of **P(2ADN)** and **P(3ADQ)** emitted in deep-blue regions with λ_{PL} at 448 nm and 453 nm, respectively. PLED devices (ITO/MoO$_3$/**P(2ADN)** or

P(3ADQ)/LiF/Al) were fabricated, but the performances were poor and no device data were reported. The authors attributed the poor efficiency to very low hole mobilities of the polymers, which were in the order of 10^{-7} and 10^{-8} cm^2 V^{-1} s^{-1}.

Wang et al. then reported a homopolymer **P(ADN)**[54] (Fig. 17) based on a known deep-blue emitter, 9,10-di(2-naphthalenyl)anthracene[55] and a series of random copolymers with styrene **P(ADN-*co*-S)** or carbazole **P(ADN-*co*-VK)** (Fig. 17). All the polymers had high T_gs (203–237°C) which did not change significantly with monomer composition. The homopolymer **P(ADN)** exhibited a deep-blue emission in tetrahydrofuran (THF) with λ_{PL} at 423 nm and 442 nm and a decent Φ_{PL} of 40%. When the compositions of styrene or carbazole increased in **P(ADN-*co*-S)** and **P(ADN-*co*-VK)**, respectively, their emission profiles became slightly blue-shifted by *ca.* 5–10 nm, suggesting the presence of chromophore aggregation in the homopolymer **P(ADN)**, similar to the aforementioned **P(2ADN)** and **P(3ADQ)**[52] (Fig. 16). This was further evidenced by the gradual Φ_{PL} increase of **P(AND-*co*-S)** from 40% to 58%, when the composition of styrene

Recent Advances in Polymer Organic Light-Emitting Diodes (PLED) Using Non-conjugated Polymers as the Emitting Layer and Contrasting Them with Conjugated Counterparts

6259

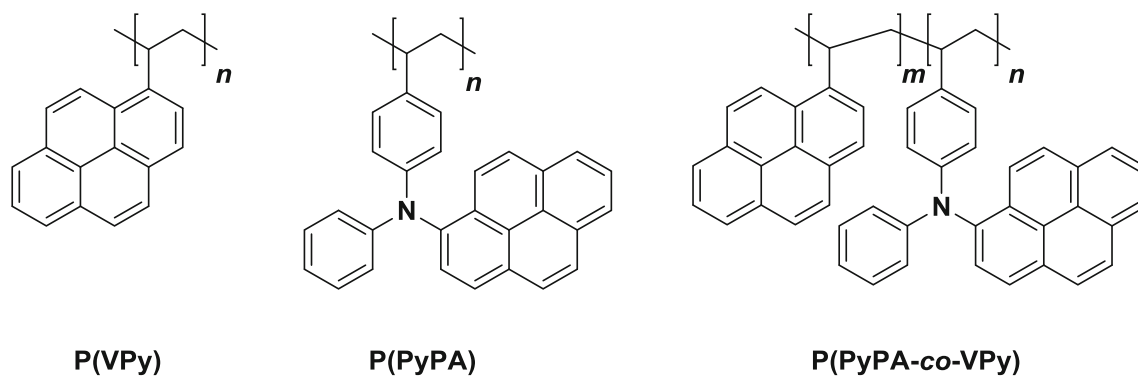**P(VPy)** **P(PyPA)** **P(PyPA-co-VPy)**

Fig. 18. Homopolymers based on pyrene, **P(VPy)**, and 1-(*N*,*N*-diphenylamino)pyrene, **P(PyPA)**, and their copolymers, **P(PyPA-co-VPy)**.

increased, which acted as a spacer and effectively prevented chromophore aggregation. However, the opposite was observed for **P(AND-co-VK)**, probably due to the stacking of the carbazole units with ADN chromophores. Indeed, pendant carbazole groups in poly(*N*-vinylcarbazole) can interact with each other in the excited state and give excimer emissions.[56] Unfortunately, the PLED device [ITO/MoO$_3$ (20 nm)/**P(ADN)**/LiF (1 nm)/Al (100 nm)] performed poorly with luminance at only *ca.* 30–50 cd m^{-2} even at applied voltage as high as 18 V. The authors attributed the poor performance to the low hole mobility (4.7×10^{-8} cm^2 V^{-1} s^{-1}) of **P(ADN)**.

Although pyrene is an efficient deep-blue emitter and has been frequently employed in OLED applications, the largely planar aromatic hydrocarbon is very prone to undesirable excimer formation.[57–60] As a result, even in very dilute solution poly (1-vinylpyrene) (**P(VPy)**, Fig. 18) shows an exclusively green emission with λ_{PL} at 491 nm and a low Φ_{PL} of 13% due to excimer emission of pyrene moieties brought into a close distance by the polymer side chain.[61] In order to solve this problem, Wang et al. prepared a novel polymer **P(PyPA)** (Fig. 18) where the propeller structure of diphenylamino group was used to induce steric hindrance around the pyrene moiety to suppress excimer formation.[61] This strategy proved to be successful so that **P(PyPA)** showed a slightly red-shifted λ_{PL} at 475 nm in THF compared with the reference compound 1-(*N*,*N*-diphenylamino)pyrene (**PyPA**, λ_{PL}: 460 nm). The Φ_{PL} of **P(PyPA)** (48%) was also comparable to that of **PyPA** (Φ_{PL}: 61%). A series of copolymers of pyrene and **PyPA**, **P(PyPA-co-VPy)** (Fig. 18), were also synthesized, and it was found that increasing pyrene content gradually red-shifted the emission, suggesting more prominent excimer formation of the pyrene moieties in the polymer. Interestingly, all the copolymers had the same Φ_{PL} of 51%. They all showed very similar T_gs (190–197°C) too. PLED devices [CFx-treated ITO/ **P(PyPA)** or **P(VPy)** or **P(PyPA-co-VPy)** (50–60 nm)/TPBI (20 nm)/LiF (1 nm)/Al (100 nm)] were fabricated and **P(PyPA)** gave the best current
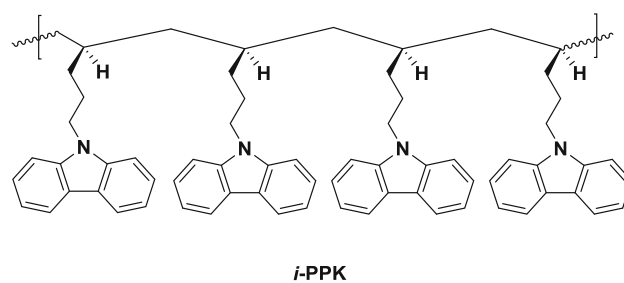

i-PPK

Fig. 19. Isotactic poly(*N*-pentyl-carbazole) (**i-PPK**) for white PLED application.

efficiency of 1.1 cd A^{-1}, but with a green λ_{EL} at *ca.* 521 nm.

Tacticity controls the stereoregularity of the polymer and its interchain stacking behaviours and, hence, can be important in PLED. For example, syndiotactic poly(diphenylaminostyrene) was found to exhibit higher hole drift mobility than isotactic ones.[62] Botta and co-workers prepared an isotactic poly(*N*-pentyl-carbazole) (**i-PPK**, Fig. 19) by a homogeneous Ziegler-Natta catalytic system of *rac*-[(CH$_3$)$_2$Si(indenyl)$_2$]ZrCl$_2$ and methylallumoxane (MAO) in toluene at 20°C.[63] Interestingly, **i-PPK** film showed a broad emission spectrum from 350 nm to 600 nm, probably due to the presence of singlet and triplet excimers similar to the case of poly(*N*-vinylcarbazole).[56] Given the broad emission, **i-PPK** was an ideal candidate for white PLED device [ITO/PEDOT:PSS (40 nm)/**i-PPK** (70 nm)/ BCP (10 nm)/Alq$_3$ (10 nm)/Ca (30 nm)/Al (70 nm)] which gave a broad electroluminescence spectrum covering from 400 nm to 800 nm with three peaks at 420 nm, 520 nm, and 620 nm. However, the efficiency was low and no numerical data were reported.

Cappelli et al. reported two interesting π-stacked polybenzofulvenes decorated with triphenylamine donor for PLED applications (**Poly-6-TPA-BF3 k** and **Poly-4'-TPA-6-MO-BF3 k**, Fig. 20).[64] Other similar π-stacked polymers include poly(dibenzoful-vene)s[65–67] and polyvinylsilafluorene[68] which have been applied in organic field-effect transistor and

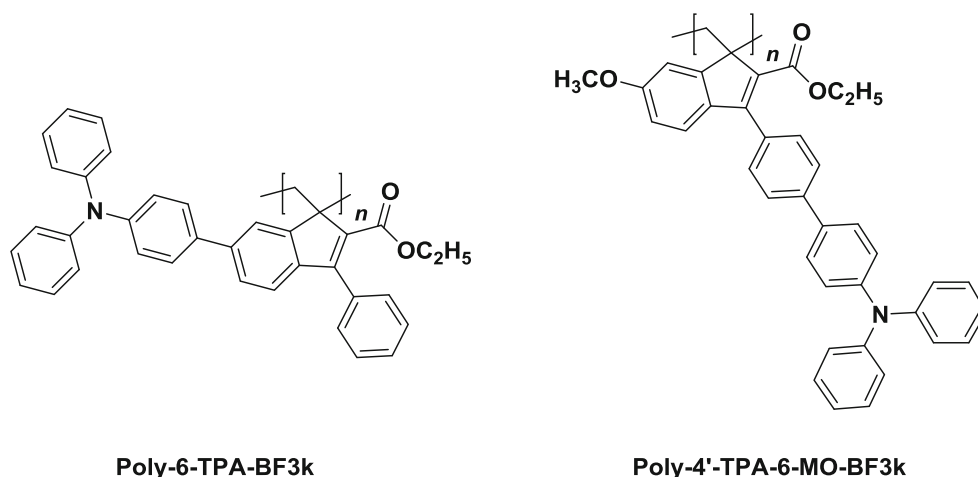**Poly-6-TPA-BF3k**   **Poly-4'-TPA-6-MO-BF3k**

Fig. 20. Two π-stacked polybenzofulvenes decorated with triphenylamine donor (**Poly-6-TPA-BF3 k** and **Poly-4'-TPA-6-MO-BF3 k**) for PLED applications.

nanofuse applications, respectively, but not in PLEDs. An unusual spontaneous polymerization (repeated concentration of monomer solutions in chloroform under reduced pressure for five times, then precipitation in ethanol) was employed to produce **Poly-6-TPA-BF3 k** and **Poly-4'-TPA-6-MO-BF3 k** which had high M_n of 233 kDa and 353 kDa as well as PDI of 2.6 and 2.7, respectively. Neat films of **Poly-6-TPA-BF3 k** and **Poly-4'-TPA-6-MO-BF3 k** showed λ_{PL} at 542 nm and 478 nm with Φ_{PL} of 23% and 9%, respectively. PLED devices [ITO/PEDOT:PSS (50 nm)/**Poly-6-TPA-BF3 k** (210 nm) or **Poly-4'-TPA-6-MO-BF3 k** (214 nm)/Ba (8 nm)/Al (70 nm)] gave poor EQEs of 0.008% and 0.0015%, respectively.

Most of the non-conjugated fluorescent polymers in this survey performed poorly in PLED devices. One main reason is their inability to utilize dark triplet excitons in the device, which constitute as large as 75% of total excitons. Thanks to the recent advances of thermally activated delayed fluorescence (TADF) mechanism[69–72] (*vide infra*) which allow purely organic materials to recruit dark triplets and ,hence, achieve 100% IQE, it is expected that the 1st generation fluorescent emitters will soon fade.

Thermally Activated Delayed Fluorescence (TADF) Polymers

TADF is the third generation OLED mechanism, which utilizes the dark triplet excitons by thermally up-converting them to emissive singlet excitons via reverse intersystem-crossing (RISC) as a result of a vanishingly small energy gap (ΔE_{ST}) between the lowest singlet state (S_1) and the lowest triplet state (T_1).[69–72] The key merit of the TADF mechanism is to allow purely organic emitters made of light elements (C, H, O, N etc.) to achieve comparable EQE (20–30%) to the expensive second generation phosphorescent emitters made of rare heavy metals
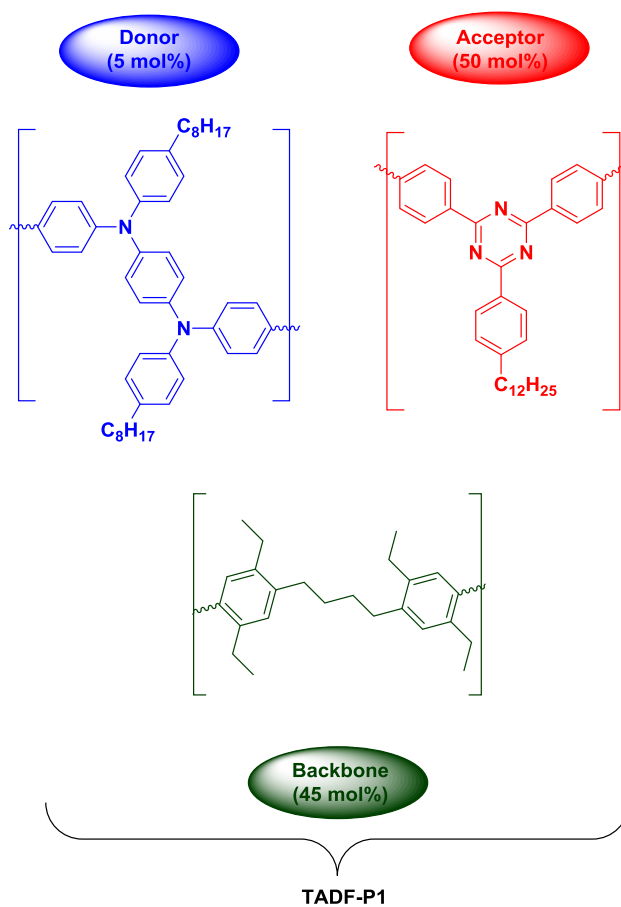

Fig. 21. Composition of the first TADF polymer (**TADF-P1**) which consists of 5 mol.% triphenylamine donor, 50 mol.% 1,3,5-triazine acceptor and a 45 mol.% backbone with an insulating *n*-butyl linkage. Adapted with permission from Ref. 77. Copyrighted by Wiley.

such iridium and platinum.[69,70,72] Currently, the vast majority of TADF emitters are small molecules with devices that were fabricated by the costly

Recent Advances in Polymer Organic Light-Emitting Diodes (PLED) Using Non-conjugated
Polymers as the Emitting Layer and Contrasting Them with Conjugated Counterparts
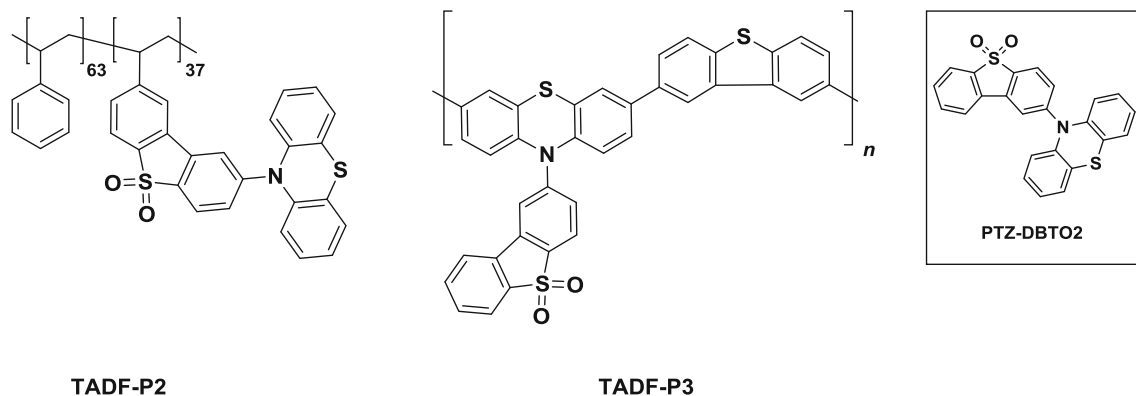
6261

Fig. 22. Chemical structures of non-conjugated and conjugated TADF copolymers (**TADF-P2** and **TADF-P3,** respectively) reported by Nobuyasu and co-workers. Also shown in the inset is the prototypical TADF emitter **PTZ-DBTO2**. Adapted with permission from Refs. 21 and 80. Copyrighted by the American Chemical Society and Wiley.

vacuum thermal evaporation technique[69,70,72] with a few exceptions.[73–75] Polymeric emitters, on the other hand, are solution-processable and enjoy more facile device fabrication procedure.

Unexpectedly, it took 4 years after the pioneering study of the organic TADF emitter in 2011[76] for the first TADF polymer to be reported by Nikolaenko and co-workers who prepared **TADF-P1**[77] (Fig. 21) with a TADF chromophore that is very similar to that of **DPA-TRZ**[78] reported by Shizu and co-workers. The polymer consists of 5 mol.% triphenylamine donor, 50 mol.% 1,3,5-triazine acceptor and a 45 mol.% backbone unit with an insulating n-butyl linkage. The much higher composition of the 1,3,5-triazine acceptor serves to balance the hole and electron mobilities of the polymer so that the recombination zone could be located near the center of the polymeric emitting layer. The insulating n-butyl linkage in the backbone unit is important because it limits conjugation length to avoid generating triplet traps in the polymer.[79] The polymer neat film showed λ_{PL} at 540 nm and Φ_{PL} of 44%, with a considerably small ΔE_{ST} of 0.22 eV. PLED device [ITO (45 nm)/PEDOT:PSS (65 nm)/interlayer (40 nm)/**TADF-P1** (80 nm)/NaF (2 nm)/Al (100 nm)/ Ag (100 nm)] gave a green λ_{EL} at ~530 nm and CIE at (0.32, 0.58) with an EQE of 10.0%. Yet, the authors did not report any characterization data (nuclear magnetic resonance (NMR) spectroscopy, infrared (IR) spectroscopy, gel-permeation chromatography (GPC), etc.) of their polymer.

Nobuyasu et al. designed a novel TADF emitter **PTZ-DBTO2** (Fig. 22) whose crystal structure showed a nearly perpendicular arrangement between the phenothiazine donor and the dibenzosulfone acceptor moieties.[80] As a result, the HOMO and LUMO are largely separated, resulting in a ΔE_{ST} as small as 0.018 eV. Two different types of copolymers, non-conjugated **TADF-P2** (copolymerized with styrene, Fig. 22) and conjugated **TADF-P3** (copolymerized with dibenzothiophene, Fig. 22), containing the **PTZ-DBTO2** chromophore, were synthesized. Both

TADF-P2 and **TADF-P3** neat films showed λ_{PL} at 565 nm but the authors did not report any Φ_{PL} data of **PTZ-DBTO2** and the two copolymers. Indeed, the absorption of **PTZ-DBTO2** in toluene showed little sign of intramolecular charge-transfer (ICT) contribution, suggesting very limited overlap between the frontier molecular orbitals, which should result in a small transition dipole moment and, hence, a slow radiative rate constant (k_r).[78,81] **TADF-P2** was applied as a dopant in the small-molecule CBP host (10 wt.%) while **TADF-P3** also doped in PBD and PVK at a weight ratio of 1:4:5. Devices of **TADF-P2** [ITO/PEDOT:PSS (40 nm)/10 wt.% **TADF-P2** in CBP (25 nm)/TPBi (50 nm)/LiF (1 nm)/Al (100 nm)] and **TADF-P3** [ITO/PEDOT:PSS (40 nm)/10 wt.% **TADF-P3** and 40 wt.% PBD in PVK (25 nm)/TPBi (50 nm)/LiF (1 nm)/Al (100 nm)] gave EQEs of 2.3% and 11.1%, respectively, but no information about the emission colors was given.

A follow-up study by the same group investigated the impact of styrene content in a series of copolymers of styrene and **PTZ-DBTO2** chromophore on their photophysical properties and device performance.[21] A homopolymer of **PTZ-DBTO2** was also synthesized and studied. It was found that, with increasing styrene composition in the polymers, the contribution of the delayed fluorescence became more significant due to suppressed triplet-triplet annihilation (TTA) because the concentration of **PTZ-DBTO2** chromophore in the polymer was diluted. Polymer with the lowest **PTZ-DBTO2** composition (37 mol.%, i.e., **TADF-P2**) exhibited the smallest ΔE_{ST} of 0.35 eV, while other polymers (46 mol.%, 67 mol.%, and 100 mol.% **PTZ-DBTO2**) had larger values (0.40–0.46 eV). Again, no Φ_{PL} data were reported. Similar to their previous study,[80] all the polymers were doped in a small-molecule host (10 wt.%) but this time mCP was employed due to its much higher triplet energy (2.9 eV) than that of CBP (2.56 eV) in order to confine triplet excitons on the **PTZ-DBTO2** chromophore so that undesirable TTA and host
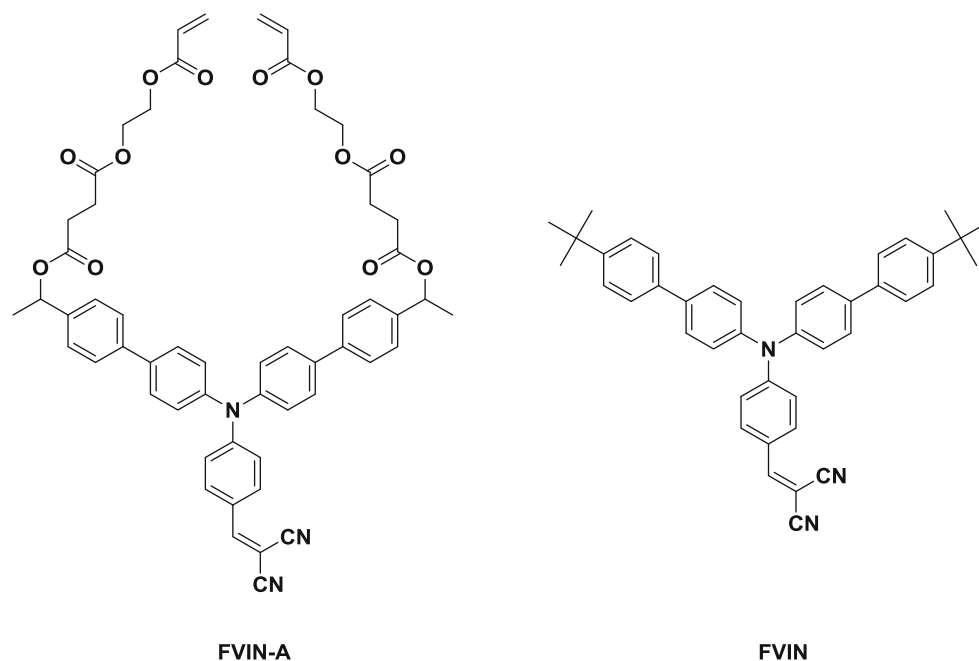
Fig. 23.   Chemical structures of cross-linkable orange-red emitter **FVIN-A** and its noncross-linkable reference **FVIN**.

quenching could be minimized. Device (ITO/PED-OT:PSS (40 nm)/10 wt.% **TADF-P2** in mCP (45 nm)/TPBi (30 nm)/LiF (1 nm)/Al (100 nm) exhibited the highest EQE of 20.1% among all polymers, which was far better than using CBP as host (EQE: 2.3%).[80] As expected, the device EQEs showed a clear positive correlation with styrene content. For example, the homopolymer of **PTZ-DBTO2** chromophore gave a low EQE of 1.4% only.

The best performing non-conjugated TADF polymer in this review is **TADF-P2** with a device that gave an EQE of 20.1%,[21] yet it should be noted that the polymer was doped in a large amount (90 wt.%) of small-molecule mCP host as the emitting layer. On the other hand, neat **TADF-P1** as the emitting layer gave a decent EQE of 10%.[77] Intuitively, TADF polymers should be based on a non-conjugated back-bone to prevent triplet trap formation as triplet energy has been known to decrease rapidly with increasing effective conjugation length.[79,82] However, there have been several reports of conjugated TADF polymers with chromophores either grafted[83,84] or built-in along the polymer main-chain[85–87,] and most of them per-formed nicely in PLED devices (EQE: 2.2–16.1%). Wei et al. recently demonstrated how a TADF-inactive carbazole-based monomer could be turned into a TADF-active macromolecule (macrocycle or poly-mer).[88] These results suggest that TADF polymers can be constructed with either conjugated or non-conjugated backbones, and they perform equally well.

Cross-Linked Polymers

Much research effort has been devoted to all-solution-processed devices (i.e., every organic layer in the device is deposited by a wet process) to significantly reduce fabrication cost.[89,90] However, the main obstacle is the dissolution of the previous organic layer by the solvent used for the deposition of the current layer. One resolution is to first spin-cast cross-linkable materials on the substrate fol-lowed by thermal-[91] or photo-induced[92,93] cross-linking so as to transform them into an insoluble polymeric layer. The main advantage of the cross-linking approach over other methods such as use of orthogonal solvent[94] and polyelectrolyte route[95] is that the intractable cross-linked layer is resistant to all organic solvents. On the other hand, in some cases thermal- or photo-induced cross-linking can cause damage to the organic materials of the device.[92]

Derue et al. prepared a cross-linkable orange-red emitter **FVIN-A** (Fig. 23) which generated an excel-lent film after ultraviolet irradiation with a R_q (root-mean-square surface roughness) as low as 0.7 nm.[92] The film showed a λ_{PL} at 635 nm with a high Φ_{PL} of 37%. An all-solution-processed device [ITO/PED-OT:PSS (40 nm)/QUPD (35 nm)/**FVIN-A** (25 nm)/TPBI (50 nm)/LiF (1 nm)/Al (100 nm)] showed λ_{EL} and CIE at 600 nm and (0.54, 0.45), respectively, where QUPD is a commercial cross-linkable hole-transporting material first reported by Yang and co-workers.[96] A rather weak EQE of 0.30% was obtained, which is attributed to low density of electroactive content in the cross-linked **FVIN-A** film due to its incomplete photopolymerization, and; therefore, charge transport in the film was seriously hampered. A reference device with thermally depos-ited **FVIN** and TPBI layers with identical device architecture and thickness showed similar
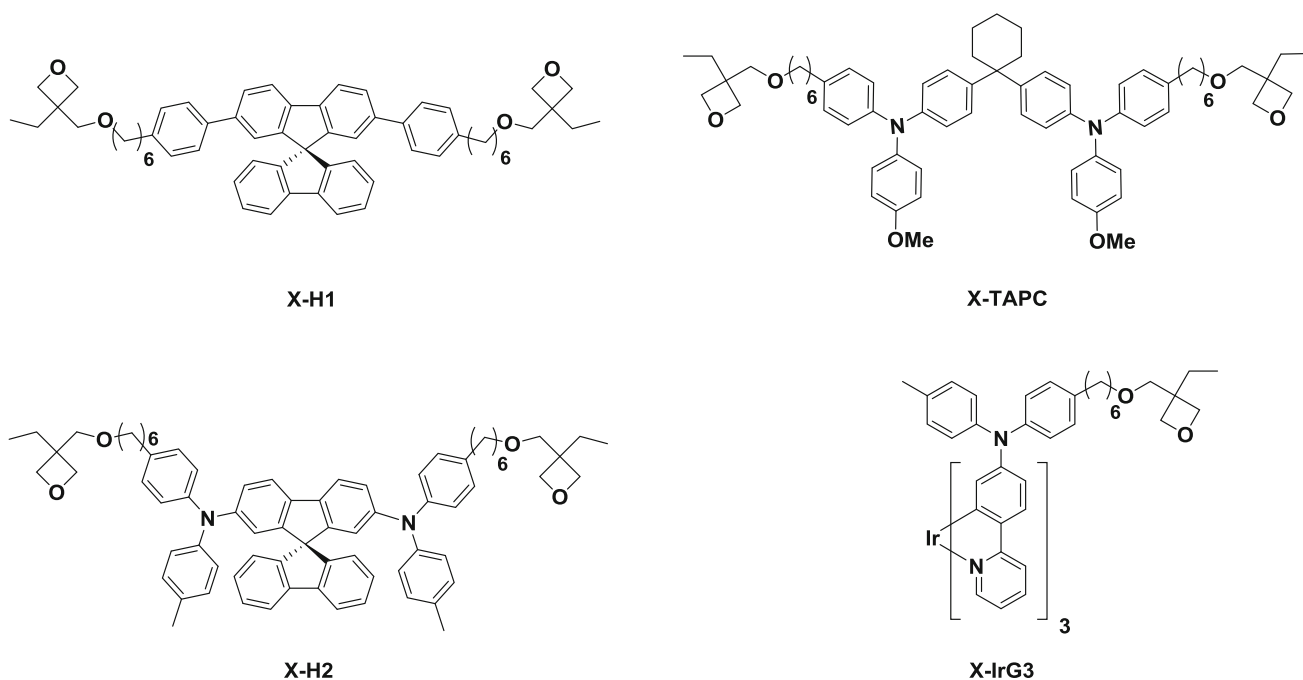
Recent Advances in Polymer Organic Light-Emitting Diodes (PLED) Using Non-conjugated
Polymers as the Emitting Layer and Contrasting Them with Conjugated Counterparts

6263

X-H1

X-TAPC

X-H2

X-IrG3

Fig. 24. Chemical structures of **X-H1**, **X-H2**, **X-TAPC** and **X-IrG3**.
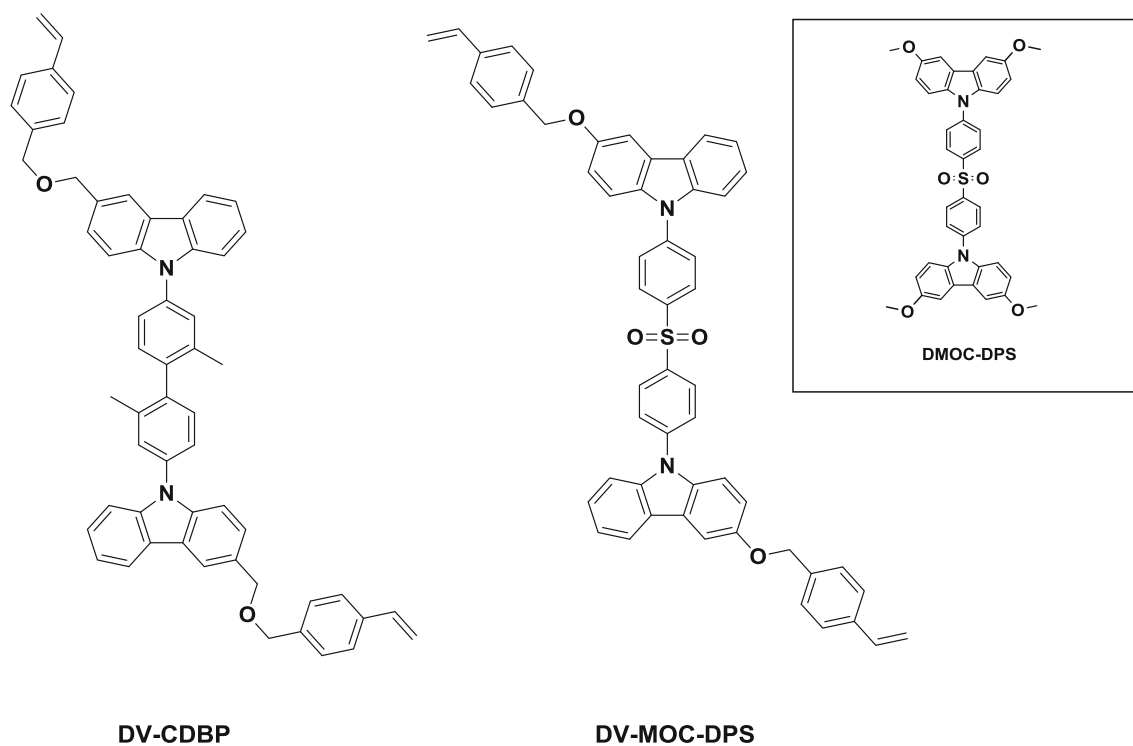
DV-CDBP

DV-MOC-DPS

DMOC-DPS

Fig. 25. Chemical structures of cross-linkable monomers **DV-CDBP** (as host) and **DV-MOS-DPS** (as TADF chromophore). Also shown in the inset is the **DMCO-DPS** prototype.[97] Adapted with permission from Refs. [91] and [97]. Copyrighted by the Royal Society of Chemistry.

efficiency (EQE: 0.37%) to the all-solution-processed analogue.

Liaptsis and co-workers applied the "double-emission layers" (DEL) strategy in their all-solution-processed phosphorescent device.[93] In DEL design, two emitting layers with different hosts are fabricated adjacent to each other so that charge carriers can be confined at their interface in order to prevent exciton leakage into other undoped layers. Two cross-linkable hosts (**X-H1** and **X-H2**, Fig. 24)
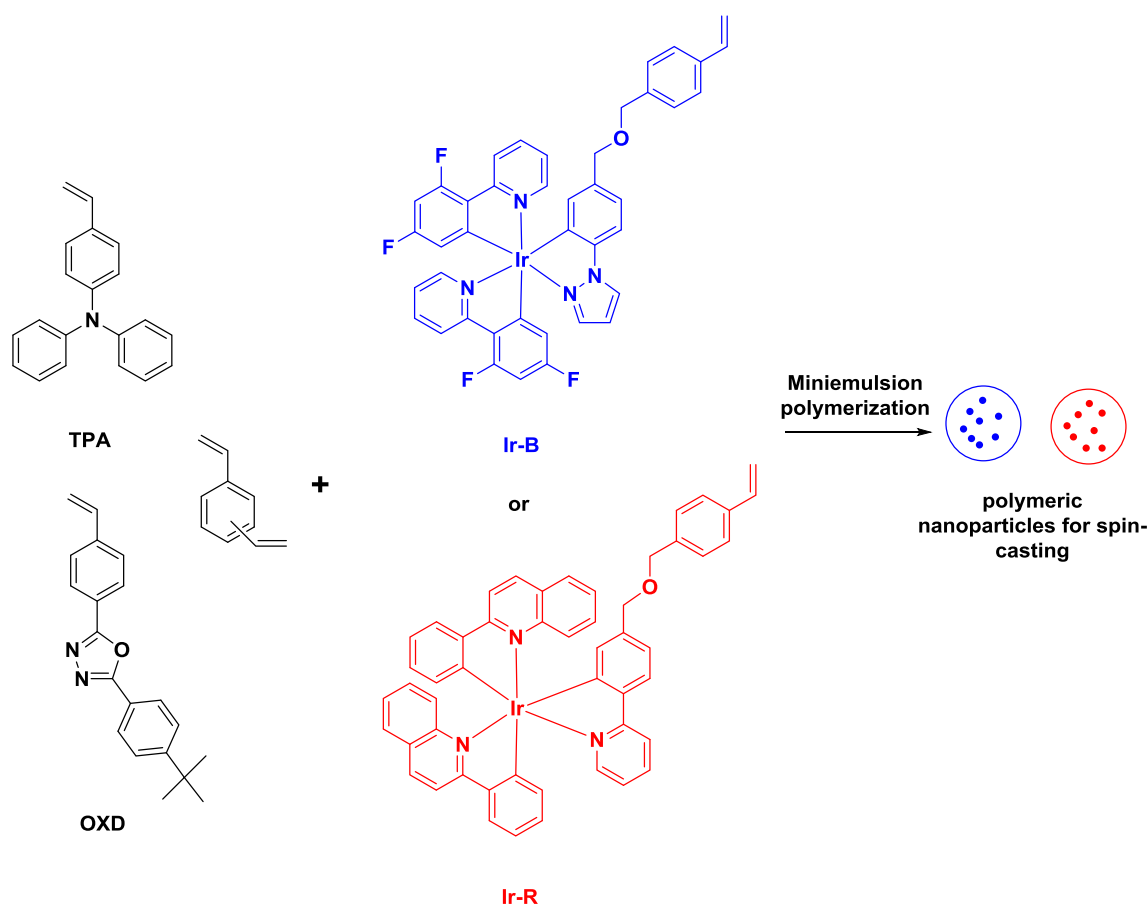
Fig. 26. The preparation of blue and red phosphorescent polymeric particles by miniemulsion copolymerization to achieve site isolation for white OLED application.

and phosphor (**X-IrG3,** Fig. 24) functionalized with oxetane groups were prepared. Doped films of **X-IrG3** (8 wt.%) in **X-H1** and **X-H2** showed excellent Φ_{PL} of 86% and 90%, respectively, under excitation at 355 nm. All-solution-processed device [ITO/PEDOT:PSS (35 nm)/X-TAPC (10 nm)/8 wt.% **X-IrG3:X-H2** (20 nm)/8 wt.% **X-IrG3:X-H1** (20 nm)/TPBI (40 nm)/CsF (2 nm)/Al (100 nm)] gave a green-yellow λ_{EL} at 530 nm and a shoulder at *ca.* 570 nm with a maximum current efficiency of 33.5 cd A^{-1}. Devices employing a single emission layer with **X-H1** and **X-H2** as hosts gave comparable maximum current efficiencies of 29.1 cd A^{-1} and 34.4 cd A^{-1} respectively.

Sun et al. prepared a cross-linkable deep-blue thermally activated delayed fluorescence (TADF) emitter **DV-MOC-DPS**[91] derived from the **DMOC-DPS**[97] prototype reported by Adachi's group (Fig. 25). A cross-linkable host **DV-CDBP** with a high triplet energy of 2.95 eV to prevent back energy transfer from the deep-blue dopant was also synthesized. It was found that cross-linked film of 9 wt.% **DV-MOC-DPS:DV-CDBP** exhibited the highest Φ_{PL} of 71% among other ratios (6 wt.% and 12 wt.%) and the film also showed an excellent surface quality with a small R_q of 0.6–0.7 nm. The

PLED device [ITO/PEDOT:PSS (30 nm)/9 wt.% **DV-MOC-DPS:DV-CDBP** (50 nm)/TPBI (40 nm)/ CsCO$_3$ (2 nm)/Al (100 nm)] exhibited λ_{EL} at 444 nm with an EQE of 2.0%.

Gao and co-workers achieved emitter site isolation for white phosphorescent OLED by cross-linked nanoparticles to suppress undesirable energy transfer from blue to red phosphor.[98] An important advantage of cross-linked nanoparticles over non-cross-linked ones is that the former can be stored in a dry state without losing particle shape, which is not possible for the latter that must be stored in aqueous dispersion to preserve the shape. Free-radical copolymerization of TPA, OXD, **Ir-B** or **Ir-G** and divinylbenzene cross-linker at a weight ratio of 1:1:10%:8% in a miniemulsion system afforded the blue- and red-emitting polymeric nanoparticles (Fig. 26). An emitting layer consisting of blue and red nanoparticles together with a linear co-polymer P(TPA-co-OXD) at a weight ratio of 3:1:4 offered a near white device [ITO/PEDOT-PSS (40 nm)/emitting layer (65 nm)/BCP (40 nm)/LiF (1 nm)/Al (100 nm)] with CIE at (0.40, 0.42) and an EQE of ~1%.

Wettach and co-workers fabricated an all-solution-processed deep-blue OLED using cross-linkable

Recent Advances in Polymer Organic Light-Emitting Diodes (PLED) Using Non-conjugated Polymers as the Emitting Layer and Contrasting Them with Conjugated Counterparts
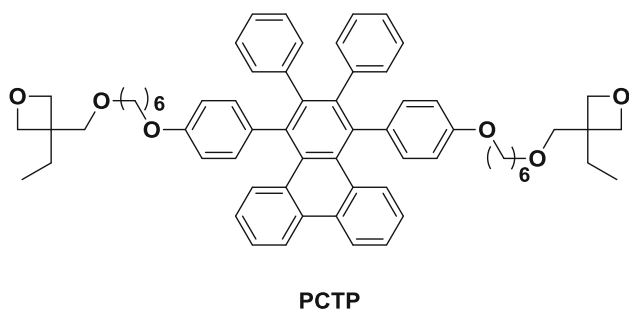
6265

PCTP

Fig. 27. Chemical structure of cross-linkable deep-blue emitter based on triphenylene moiety (**PCTP**).

emitter based on triphenylene chromophore (**PCTP**, Fig. 27).[99] The device [ITO/PEDOT:PSS (35 nm)/ QUPD (20 nm)/OTPD (10 nm)/**PCTP** (80 nm)/Ba (4 nm)/Al (150 nm)] exhibited λ_{EL} at 456 nm, but the blue emission was contaminated by a broad low-energy emission extended up to 800 nm with peaks at ~600 nm and ~750 nm, which is attributed to exciton leakage to the adjacent OTPD layer (a cross-linkable hole-transporting material reported by Yang and co-workers).[96] The efficiency of the device was poor, which reached a current efficiency of ~0.2 cd A^{-1} at most, probably due to the low emission capability of the **PCTP** emitter (Φ_{PL}: 3% in DCM).

While cross-linkable materials enable all-solution-processed devices to reduce fabrication cost, most devices based on these materials showed poorer performance than their polymer analogues. For example, a device based on cross-linked phosphor **X-IrG3** gave a current efficiency of 34.4 cd A^{-1} in the green-yellow region[93] and that using cross-linked phosphorescent nanoparticles **Ir-B** and **Ir-G** resulted in a low EQE of ~1%,[98] those efficiencies being lower than the best EQE obtained from the phosphorescent copolymer **DDIr-P1-co-VK**[30] (EQE: 14.7%).* In addition, the device based on cross-linked **DV-CDBP** (as host) and **DV-MOS-DPS** (as TADF chromophore) gave an EQE of 2.0% whereas TADF polymer **TADF-P2** offered a much higher EQE of 20.1%.[21] One possible reason for the lower device efficiency is the very limited characterization and purification available for the resulting intractable cross-linked polymer film.

CONTRASTING CONJUGATED POLYMERS WITH NON-CONJUGATED COUNTERPARTS FOR PLED APPLICATIONS

Polymers employed in PLED applications can be constructed with either conjugated or non-conjugated backbones. Both of them have been widely employed, but a systematic comparison between

these two classes of materials is rarely attempted. An understanding on the similarities and differences between conjugated polymers and non-conjugated counterparts is essential to the workers in the field when it comes to design of the desired polymers for PLED applications. Moreover, knowledge about structure-property relationship PLED polymers can be reinforced.

Conjugated versus Non-conjugated Polymers: Material Preparations

There are several important parameters for the synthesis of polymers. Polymerization yield is obviously the integral factor for the economy of the polymer. The number-average molecular weight (M_n) is a critical property that impacts the practical applications of the polymer. According to the well-known Mark-Houwink equation[123]:

$$\mu = K \times M_w^a, \tag{1}$$

where μ and M_w refer to viscosity of the polymer solution and weight-average molecular weight of the polymer, respectively. K and a are both constants, where the former is related to polymer species, temperature as well as solvent and the latter to polymer conformation. A high molecular weight is important to attain sufficient viscosity of the polymer solution for generating high-quality thin film.[32] Conjugated polymers with higher molecular weight are shown to have better charge mobility because long polymer chains serve as interconnections between ordered phases of the polymer film.[124] In addition, high-molecular-weight alternating copolymer of fluorene and MeH-PPV showed a much higher Φ_{PL} of 61.2% than the low molecular weight analogue (Φ_{PL}: 26.8%) whose short polymer chains were more rod-like, which resulted in more pronounced π-π stacking and hence greater energy transfer to the quenching site.[123] Under certain circumstances, a high-molecular-weight polymer is not necessarily superior to a low-molecular-weight one, but workers can make a wise use of their different physical properties. For instance, Al-Attar and Monkman fabricated an all-solution processed OLED device, in which a low-molecular-weight poly(N-vinylcarbazole) doped with Ir(ppy)$_3$ as the emitting layer, was spun-coated on a high-molecular-weight poly(N-vinylcarbazole) which functioned as the hole transport electron blocking layer.[125] Undesirable interlayer mixing during the fabrication of the low-molecular-weight poly(N-vinylcarbazole) was prevented because the dissolution of the high-molecular-weight poly(N-vinylcarbazole) in toluene (spin-coating solvent) was very slow. Polydispersity index (PDI) has a significant impact on the effective conjugation length homogeneity of the polymer chains which in turn affects the emission colors, formation of undesirable charge traps and interchain packing in the polymer.[33,126,127]

---

*In general, current efficiency in the green-yellow region can be roughly approximated into EQE by dividing by a factor of 3 to 4. See Refs. 85 and 100–102.

Table I. Summary of polymerization method, yield, M_n and PDI of the non-conjugated polymers reported recently (2010–present)
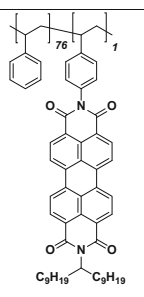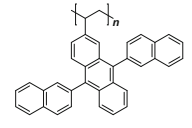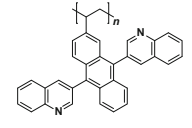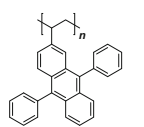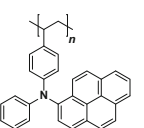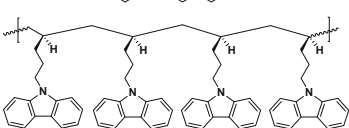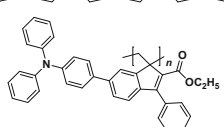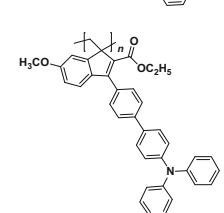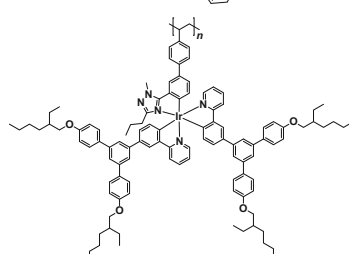
Polymer	Structure	Category	Polymerization type	Yield (%)	M_n (kDa)	PDI	Purity check	Ref.
PS-PERY-16		Fluorescent	Nitroxide Mediated Polymerization	45	32.1	1.4	–	51
P(2ADN)		Fluorescent	Free radical	85	21.5	2.3	–	52
P(3ADQ)		Fluorescent	Free radical	72	15.4	2.7	–	52
P(ADN)		Fluorescent	Free radical	68	29.1	2.1	–	54
P(PyPA)		Fluorescent	Free radical	86	7.7	2.2	–	61
i-PPK		Fluorescent	Ziegler-Natta	30	–	–	–	63
Poly-6-TPA-BF3k		Fluorescent	Spontaneous polymerization	81	233	2.6	–	64
Poly-4'-TPA-6-MO-BF3k		Fluorescent	Spontaneous polymerization	81	353	2.7	–	64
DIr-P1		Phosphorescent	Free radical	86	5.8	3.8	EA	26

Table I. continued
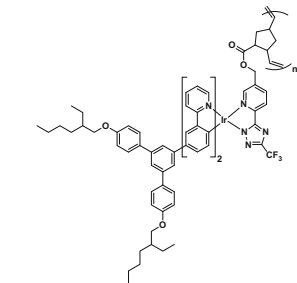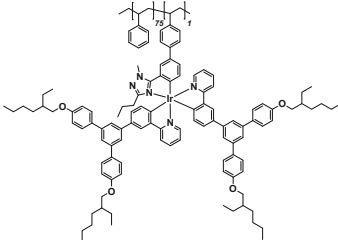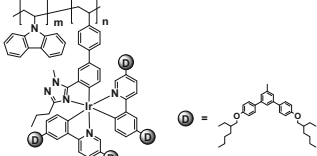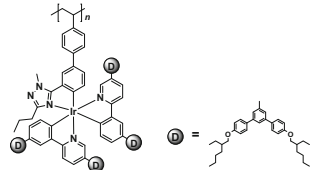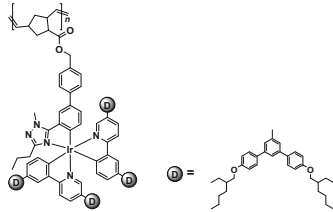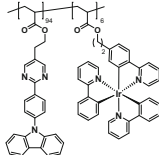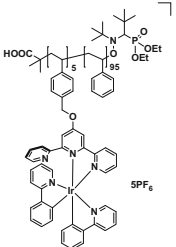
DIr-P2		Phosphorescent	Ring Opening Metathesis	72	22	2.2	−	27
DIr-P1-*co*-S		Phosphorescent	Free radical	50	7.3	1.8	−	29
DDIr-P1-*co*-VK		Phosphorescent	Free radical	81	3.3	2.3	−	30
DDIr-P1		Phosphorescent	Free radical	92	5	4	EA	31
DDIr-P3		Phosphorescent	Ring Opening Metathesis	94	47.4	1.4	EA	32
Poly(M6-MA-co-Ir-2C-MA)		Phosphorescent	Free radical	78	35	2.2	−	35
Ir-P4-5		Phosphorescent	Nitroxide Mediated Polymerization	60	38.3	1.2	−	36

Table I. continued

Ir-P5-0.03		Phosphorescent	Nucleophilic aromatic substitution	55	6.9	1.5	–	42
Ir-P5-0.075-0.007		Phosphorescent	Nucleophilic aromatic substitution	45	–	–	–	44
Ir-P6(mCP-*co*-B)		Phosphorescent	Vinyl addition	37	163	2.8	–	45
Ir-P7(10B-*co*-1R-100)		Phosphorescent	Nitroxide Mediated Polymerization	–	100	1.4	–	46
TADF-P1		TADF	Suzuki coupling	80	–	–	–	77
TADF-P2		TADF	Free radical	85	6.8	1.7	–	80

Table II. Summary of polymerization method, yield, M_n and PDI of the conjugated polymers reported recently (2011–present)
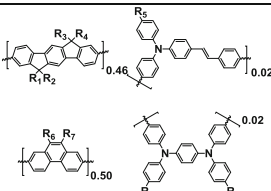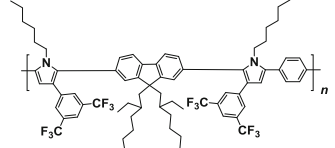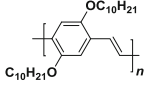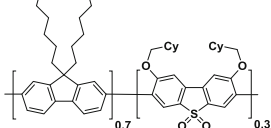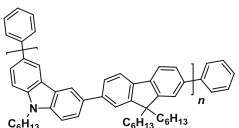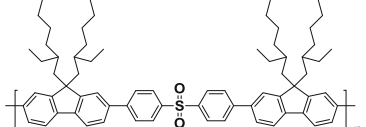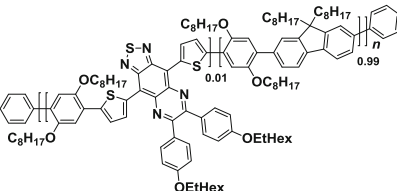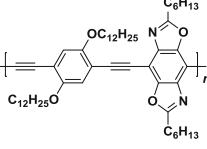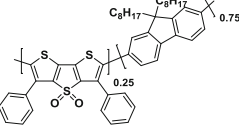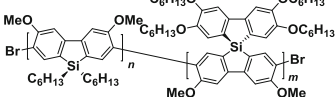
Polymer	Structure	Category	Polymerization type	Yield (%)	M_n (kDa)	PDI	Purity check	Ref
CP-ABCD		Fluorescent	Suzuki coupling	–	400–500	2.8–4.0	ICP-MS	103
7caf		Fluorescent	Multicomponent coupling	81	15.8	1.9	–	104
PDOPV		Fluorescent	Wittig–Horner reaction	84	3.5	1.6	–	105
P5		Fluorescent	Suzuki coupling	–	27.2	3.3	–	106
CF1		Fluorescent	Suzuki coupling	–	10.8	2.9	–	109
PF₂DSO		Fluorescent	Suzuki coupling	84	11.0	1.3	EA	108
P2		Fluorescent	Suzuki coupling	87	72	2.4	–	109
PBOP-D		Fluorescent	Sonogashira coupling	59	33.1	1.4	–	110
P1-25		Fluorescent	Suzuki coupling	73	23.6	1.7	–	111
PHSSF-co-PDHSF		Fluorescent	Grignard metathesis	76	>50	1.8	–	112

Table II. continued

PFO-TFP		Fluorescent	Suzuki coupling	74	16.5	2.2	EA	113
			Direct arylation	81	31.5	3.5	–	114
PF-IrNiq1		Phosphorescent	Suzuki coupling	82	51.7	2.3	–	115
PCztPSiB5		Phosphorescent	Suzuki coupling	58	7.1	1.9	–	116
PF-Ir(ppy)₂(pytzph)₅-Ir(piq)₂(pytzph)₅		Phosphorescent	Suzuki coupling	64	10.4	2.1	–	117
P-R-3		Phosphorescent	Suzuki coupling	84	31	2.0	–	118
PCz6G0		Phosphorescent	Suzuki coupling	–	25	2.1	EA	119

Recent Advances in Polymer Organic Light-Emitting Diodes (PLED) Using Non-conjugated
Polymers as the Emitting Layer and Contrasting Them with Conjugated Counterparts

6271

Table II. continued

P3		Phosphorescent	Suzuki coupling	26	9.3	1.8	−	120
pAcBP		TADF	Suzuki coupling	87	7.4	1.2	EA	85
PCzDP-10		TADF	Suzuki coupling	66	4.6	1.8	EA	83
P12		TADF	Suzuki coupling	47	3.3	1.8	EA	84
PAPTC		TADF	Suzuki coupling	84	22.0	3.0	−	86
FCP 2.5		AIE	Suzuki coupling	83	21.0	2.3	−	121
FBPAN 0.5		AIE	Suzuki coupling	83	9.0	1.6	−	122

Table III. Summary of PLED performances based on non-conjugated polymers, their PLQY (Φ_{PL}), glass-transition temperature (T_g) and film surface roughness (R, where R_a and R_q refer to average and root-mean-squared roughness, respectively)

Polymer	Structure	Category	Φ_{PL} (%)	T_g (°C)	R (nm)	λ_{EL} (nm)	EQE (%)	Ref
P(2ADN)		Fluorescent	43 (THF)	343	–	–	Very weak	52
P(3ADQ)		Fluorescent	24 (THF)	298	–	–	Very weak	52
P(ADN)		Fluorescent	40 (THF)	237	–	–	Very weak	54
P(PyPA)		Fluorescent	61 (THF)	190	–	~520	– (1.1 cd A^{-1})	61
i-PPK		Fluorescent	–	90	0.6 (R_a)	~420, ~520, ~620 (white)	Very weak	63
Poly-6-TPA-BF3k		Fluorescent	23 (neat)	–	–	–	0.008	64
Poly-4'-TPA-6-MO-BF3k		Fluorescent	9 (neat)	–	–	–	0.0015	64
DIr-P1		Phosphorescent	42 (20 wt.% in CBP)	Not observed	0.24 (R_a)	520	7.5	26
DIr-P2		Phosphorescent	52 (20 wt.% in CBP)	Not observed	–	~525	5.1	27

Recent Advances in Polymer Organic Light-Emitting Diodes (PLED) Using Non-conjugated
Polymers as the Emitting Layer and Contrasting Them with Conjugated Counterparts

6273

Table III. continued
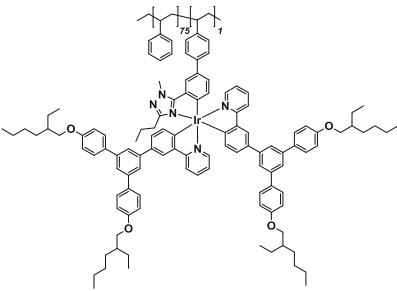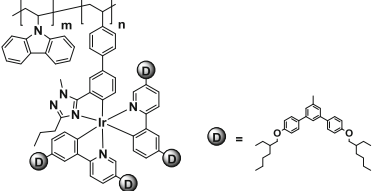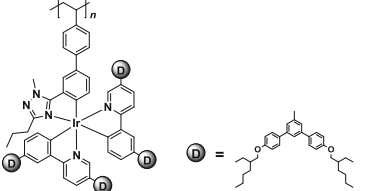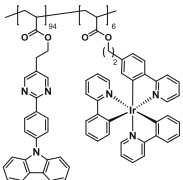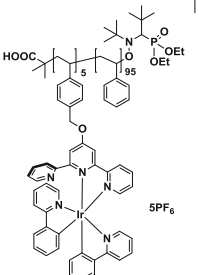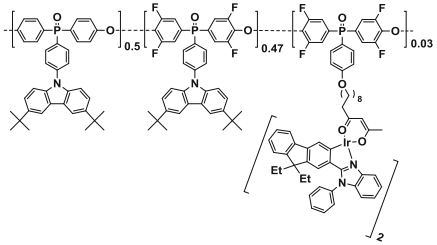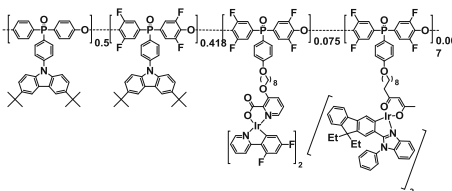
Name	Type						
DIr-P1-*co*-S	Phosphorescent	67 (20 wt.% in CBP)	–	–	517	6.7	29
DDIr-P1-*co*-VK	Phosphorescent	73 (50 wt.% in CBP)	–	–	545	14.7	30
DDIr-P1	Phosphorescent	47 (neat)	–	–	~550, ~600 (sh)	9.2	31
Poly(M6-MA-*co*-Ir-2C-MA)	Phosphorescent	65 (neat)	–	–	~ 520	– (3.6 cd A^{-1})	35
Ir-P4-5	Phosphorescent	–	–	–	–	– (max. 5 cd m^{-2})	36
Ir-P5-0.03	Phosphorescent	–	254	–	566	4.1	42
Ir-P5-0.075-0.007	Phosphorescent	–	–	–	–	(0.31, 0.43)	7.1	44

Table III. continued
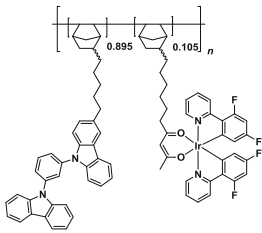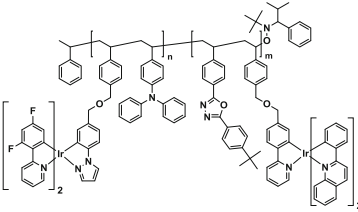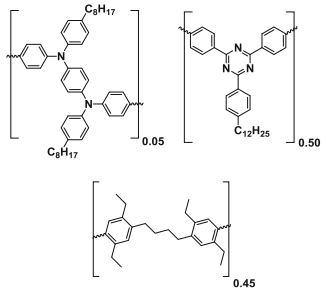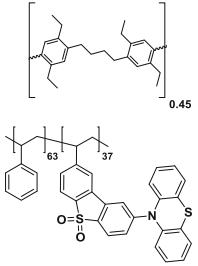
Ir-P6(mCP-*co*-B)	Phosphorescent	–	Not observed	–	488	8.8	45
Ir-P7(10B-*co*-1R-100)	Phosphorescent	–	–	–	~500, ~600 (white)	1.5	46
TADF-P1	TADF	43.6 (neat)	–	–	~540	10.0	77
TADF-P2	TADF	–	217	–	533	20.1	80

Table I summarizes the polymerization method, yield, number-average molecular weight (M_n) and polydispersity index (PDI) of the non-conjugated polymers introduced in this review. For comparison, the same information for the vast majority of conjugated polymers reported in the recent years (2011-present) is also presented in Table II. Among the 22 non-conjugated polymers, free-radical polymerization is the most widely used polymerization method, which amounts to 45.5% of all polymers synthesized due to its well-established chemistry and high functional group tolerance.[128,129] The average yields, M_n and PDI of polymers generated via free-radical polymerization are 78.3%, 14.3 kDa and 2.5, respectively. The more advanced living radical polymerization such as nitroxide-mediated polymerization (NMP) allows polymers with much lower PDIs (1.2–1.4) to be synthesized.[36,46,51] Nucleophilic aromatic substitution (SNAr) polycondensation resulted in a low M_n of 6.9 kDa yet with a decent PDI of 1.5 in a 55% yield[42] but the success of this polymerization method strongly depends on the degree of activation of the electrophilic carbon to be attacked, and; hence, its generality can be limited.[43] Vinyl addition polymerization of norbornene-based monomer offered a very high M_n of 163 kDa, but suffered from a low yield of 37% and a high PDI of 2.8.[45]

Among the 23 conjugated polymers, Suzuki coupling has dominated the polymerization method, which amounts to 79.2% of all polymers synthesized due to its well-established chemistry and employment of more environmentally benign reagents (e.g., Stille coupling is notoriously known for the toxic organotin reagents). The average yields, M_n and PDI of polymers synthesized via this method are 72.1%, 45.4 kDa and 2.2, respectively. Direct arylation polymerization (DAP) has recently attracted intense research attention, because it is more economical (fewer synthetic steps) and environmentally friendly (less organometallic by-products) than the traditional C-C bond formation chemistry.[130,131] **PFO-TFP** synthesized via DAP had a M_n and PDI of 31.5 kDa and 3.5, respectively, in an 81% yield,[114]

Recent Advances in Polymer Organic Light-Emitting Diodes (PLED) Using Non-conjugated
Polymers as the Emitting Layer and Contrasting Them with Conjugated Counterparts

6275

Table IV. Summary of PLED performances based on conjugated polymers, their PLQY (Φ_{PL}), glass-transition temperature (T_g) and film surface roughness (R, where R_a and R_q refer to average and root-mean-squared roughness, respectively)

Polymer	Structure	Category	Φ_{PL} (%)	T_g (°C)	R (nm)	λ_{EL} (nm)	EQE (%)	Ref
CP-ABCD		Fluorescent	–	–	–	459, 480 (sh)	– (9.7 cd A^{-1})	103
7caf		Fluorescent	50 (chloroform)	–	–	445	– (0.2 cd A^{-1})	104
PDOPV		Fluorescent	34 (THF)	–	–	560	<1 (0.73 cd A^{-1})	105
P5		Fluorescent	62 (neat)	–	–	~450	3.2	106
CF1		Fluorescent	20 (neat)	134	–	409	2.1	107
PF₂DSO		Fluorescent	68 (chloroform)	–	–	–	Very weak	108
P2		Fluorescent	<1 (neat)	–	–	909	0.04	109
PBOP-D		Fluorescent	57 (chloroform)	Not observed	–	501	1.1	110
P1-25		Fluorescent	12 (EtOH)	–	–	545	0.04	111
PHSSF-co-PDHSF		Fluorescent	85 (neat)	Not observed	–	410	2.9	112
PFO-TFP		Fluorescent	68 (neat)	Not observed	1.2 (R_q)	405	5.02	113
			66 (Chloroform)	Not observed	–	–	–	114

Table IV. continued

PF-IrNiq1		Phosphorescent	66 (neat)	–	–	637	7.8	115
PCztPSiB5		Phosphorescent	8.4 (neat)	–	1.30 (R_q)	473	1.73	116
PF-Ir(ppy)$_2$(pytzph)$_5$-Ir(piq)$_2$(pytzph)$_5$		Phosphorescent	19 (neat)	133	1.79 (R_q)	White (0.32, 0.34)	– (11.49 cd A^{-1})	117
P-R-3		Phosphorescent	–	125	–	640	16.1	118
PCz6G0		Phosphorescent	–	–	–	524	9.6	119
P3		Phosphorescent	77 (DCM)	79	–	560	– (2.90 cd A^{-1})	120

Recent Advances in Polymer Organic Light-Emitting Diodes (PLED) Using Non-conjugated
Polymers as the Emitting Layer and Contrasting Them with Conjugated Counterparts

6277

Table IV. continued

pAcBP		TADF	46 (10 wt.% in TCTA:TAPC)	184	0.21 (R_q)	548	9.3	85
PCzDP-10		TADF	74 (neat)	~165	–	496	16.1	83
P12		TADF	33.7 (neat)	126	0.39 (R_q)	506	4.3	84
PAPTC		TADF	28 (neat)	–	–	521	12.6	86
FCP 2.5		AIE	71.5 (neat)	–	–	White (0.33, 0.34)	– (6.34 cd A^{-1})	121
FBPAN 0.5		AIE	80.2 (neat)	73	–	White (0.32, 0.31)	– (7.56 cd A^{-1})	122

whereas the same polymer synthesized via Suzuki coupling showed a M_n and PDI of 16.5 kDa and 2.2, respectively, in a 74% yield.[113]

Both conjugated and non-conjugated polymers are economical because the majority of the two classes of polymers were obtained with >70% yields. A direct comparison of M_n and PDI between the two classes of polymers may be inappropriate, because they were not prepared by a single polymerization method. As mentioned previously, the most popular polymerization methods for conjugated and non-conjugated polymers are Suzuki coupling and free-radical polymerization, respectively, where the average M_n and PDI are 45.4 kDa and 2.2 for the conjugated polymers as well as 12.0 kDa and 2.5 for the non-conjugated polymers. While Suzuki coupling polycondensation seems to give polymers with better M_n and PDI than those produced via free-radical polymerization, it cannot be concluded that non-conjugated polymers are inferior in terms of M_n and PDI parameters. Indeed, living radical polymerization, in principle, is able to give any M_n desired based on the monomer to initiator ratio along with a very low PDI (e.g., <1.2). The analogous polymerization for conjugated polymers is the Grignard metathesis polymerization (GRIM) which

shows *quasi*-living characters and is commonly used for preparing regioregular poly(3-hexylthiophene) (P3HT).[132] Both of these polymerization methods are able to produce block copolymers.[46,133] However, strongly nucleophilic organomagnesium species is inevitably present in GRIM, which severely limit the scope of monomers that can be polymerized, whereas radical polymerization is well known to have high functional group tolerance.[128,129] Interestingly, block copolymers are unpopular in PLED applications: only one non-conjugated block copolymer was reported recently[46] and conjugated block copolymer was absent.[134,135]

A critical parameter of OLED materials is purity because impurities can act as charge trapping sites and quenchers during device operation.[136] However, among the 45 polymers (conjugated and non-conjugated) presented in this review, only ten of them had their purities verified (see "purity check" column in Tables I and II). This was done by elemental analysis (EA) techniques, and the results were essentially all based on CHN elemental compositions with only a few exceptions. For example, conjugated polymer CP-ABCD was examined by inductively coupled plasma mass spectrometry (ICP-MS) to detect trace elements like bromine, boron, phosphorus and palladium with concentrations that were found to be ≤50 ppm, ≤20 ppm, ≤200 ppm, and ≤15 ppm, respectively.[103] Giovanella et al., along with CHN analysis, performed mass spectrometry analysis to conclude the absence of residual bromine and borolane groups in their PFO-TFP polymer.[113] In addition to being unable to detect trace elements like halogens and transition metals, CHN analysis has a serious limitation, when it comes to random copolymers whose exact monomer compositions cannot be confirmed due to the broadness and overlap of aromatic peaks in the ^{1}H NMR spectra.[30,45,116] Halogenated impurities have been shown to be detrimental to the PLED device lifetime due to radical chain type degradation.[137] In addition, palladium black formed during polycondensation can be hard to remove completely.[132] Given that the vast majority of conjugated polymers are generated by transition-metal catalyzed coupling in which monomers containing aryl bromide are frequently employed, non-conjugated polymers, which are mainly synthesized by free- or living-radical polymerizations where no transition metals and halogens are involved, may have an advantage over the conjugated counterparts in this regard.

Conjugated versus Non-conjugated Polymers: PLED Performances

The PLED performance (λ_{EL} and EQE) based on non-conjugated and conjugated polymers are summarized in Tables III and IV, respectively, which also list the related determining parameters, such as the polymers' PLQY (Φ_{PL}), glass-transition temperature (T_g) and film surface roughness (R).

Among the phosphorescent PLEDs, the best performing non-conjugated polymer (DDIr-P1-*co*-VK) exhibited an EQE of 14.7% with a green emission (λ_{EL} at 545 nm)[30] while the conjugated counterpart (P-R-3) exhibited an EQE of 16.1% with a red emission (λ_{EL} at 640 nm).[118] On the other hand, the best non-conjugated TADF polymer (TADF-P2) offered a green PLED (λ_{EL} at 533 nm) with an EQE of 20.1%[21,] whereas the conjugated counterpart (PCzDP-10) gave a PLED with a blue emission at 496 nm and an EQE of 16.1%.[83] Therefore, it is reasonable to conclude that for these two classes of polymers (phosphorescent and TADF), the nature of the polymer backbone has minimal impact on the PLED performance.

However, this is not the case for the fluorescent PLEDs, where non-conjugated and conjugated polymers show a significant difference in their PLED efficiencies. For example, while the best conjugated fluorescent polymers (P5[106] and CP-ABCD[103,] respectively) offered some decent PLED efficiencies such as an EQE of 3.2% and a current efficiency of 9.7 cd A^{-1} (both in the sky-blue region), all non-conjugated fluorescent polymers exhibited much poorer PLED performance (<1 cd A^{-1}). This remarkable difference in PLED efficiencies should *not* be explained by differing determining factors such as PLQY, surface roughness, and charge carrier balance of the emitting polymer layer brought about by the nature of the polymer backbone, because the difference in the PLED efficiencies are only observed in fluorescent PLEDs but not in phosphorescent and TADF PLEDs. Indeed, the PLQYs of non-conjugated fluorescent polymers are competitive (up to 61% in THF)[61] and the surface roughness seems to not depend on the nature of the polymer backbone ($R_a < 1$ nm).[26,63] Considering the key difference between fluorescent polymers and phosphorescent/TADF analogues is the utilization of triplet excitons for emission in the latter two types of materials, one might wonder if the nature of the polymer backbone affected the exciton utilization efficiency (η_S), hence, resulting in the remarkably different PLED efficiencies demonstrated by non-conjugated and conjugated fluorescent polymers. The internal quantum efficiency (IQE) of PLED is strongly related to η_S according to the following expression[138]:

$$\text{IQE} = \Phi_{PL} \times \eta_{rec} \times \eta_S, \qquad (2)$$

where η_{rec} and η_S refer to charge recombination and exciton utilization efficiencies, respectively. In phosphorescent and TADF materials, both singlet and triplet excitons can contribute to emission and, hence, η_S equals 1. On the other hand, fluorescent materials, in principle, have their emission contributed only by singlet excitons, and; hence, η_S equals merely 0.25 according to spin statistics. However, one must be aware that in practical OLED operation, triplet excitons can also contribute

to emission in fluorescent materials due to the presence of triplet-triplet annihilation (TTA) in which two dark triplet excitons merge to form an emissive singlet exciton. Indeed, this process can be surprisingly efficient and contribute as a major emission mechanism in fluorescent PLED devices (up to 20–60% of total emission).[139,140] It follows that fluorescent polymers with a conjugated polymer backbone might undergo a more efficient TTA process than those with a non-conjugated backbone and, hence, show better PLED efficiencies. It could be that the extensive charge delocalization in the conjugated polymers may significantly lower the triplet energy level (T_1)[79,] and; hence, the triplet-polaron annihilation (TPA) and TTA processes would not be able to produce excessive energy that causes structural disruption of the emitting species, where the former has been regarded as the major degradation cause for the blue phosphorescent materials.[141] Moreover, the conjugated backbone might result in better intrachain or interchain bimolecular triplet exciton communication to allow a more efficient TTA process. Of course, it could also be that the currently reported PLED efficiencies of fluorescent polymers with non-conjugated backbone have not yet reflected the true potential of this class of materials. However, given the explosive development of TADF OLED materials in the recent years,[69,70,72] the research interest in fluorescent materials has been sharply diminished.

CONCLUSIONS

In this review, recent advances in the development of non-conjugated polymers for PLED applications have been discussed. While fluorescent non-conjugated polymers performed poorly in PLEDs, phosphorescent and TADF polymers offered much more competitive PLED devices where the efficiencies of these two classes of materials have been comparable. Based on the comparison with recently reported PLED devices using conjugated polymers, it can be concluded that phosphorescent and TADF PLED performances do not depend on whether the polymer backbone is conjugated, whereas conjugated fluorescent PLED exhibited much higher efficiencies than the non-conjugated counterparts. This might be because the conjugated polymer backbone allows better triplet exciton recruitment via the triplet-triplet annihilation (TTA) process, or because the true potential of non-conjugated fluorescent PLED has just not yet been revealed.

Further research efforts in some areas are still required. For example, the effects of molecular weight and polydispersity of the polymers on the PLED performance are still underexplored. Although a few previous studies were conducted,[33,34,126,127] much more work has to be done to gain conclusions of enhanced generalities and also to obtain more solid understanding on the structure-property relationships in PLED materials. In addition, the purity of

polymers for PLED applications should always be verified to establish a reliable link between device performances with the structure of the polymer employed in the device. However, a survey conducted in this review shows that only ten out of 45 PLED polymers had their purity verified.

As to the outlook of PLED materials, it is expected that TADF polymers will receive escalating research attention and efforts due to their lower costs and ability to utilize triplet excitons in the device. Currently, the TADF polymers reported so far were all used as the primary emitting species for the devices. In principle, TADF polymers can also be used as host materials for conventional fluorescent dyes.[69] In this setting, the host is responsible for upconversion of dark triplet excitons, which then transfers its energy to the fluorescent dopant dye which has key merits of high PLQY and much narrower emission spectrum (i.e., enhanced color purity). TADF polymers for white light emission still remain as a challenge. While the current progress of PLED materials has been very fruitful and encouraging, further research efforts are still required.

OPEN ACCESS

This article is distributed under the terms of the Creative Commons Attribution 4.0 International License (http://creativecommons.org/licenses/by/4.0/), which permits unrestricted use, distribution, and reproduction in any medium, provided you give appropriate credit to the original author(s) and the source, provide a link to the Creative Commons license, and indicate if changes were made.

ELECTRONIC SUPPLEMENTARY MATERIAL

The online version of this article (doi: 10.1007/s11664-017-5702-7) contains supplementary material, which is available to authorized users.

REFERENCES

1. C.W. Tang and S.A. VanSlyke, *Appl. Phys. Lett.* 51, 913 (1987).
2. T.-A. Lin, T. Chatterjee, W.-L. Tsai, W.-K. Lee, M.-J. Wu, M. Jiao, K.-C. Pan, C.-L. Yi, C.-L. Chung, K.-T. Wong, and C.-C. Wu, *Adv. Mater.* 28, 6976 (2016).
3. H. Kaji, H. Suzuki, T. Fukushima, K. Shizu, K. Suzuki, S. Kubo, T. Komino, H. Oiwa, F. Suzuki, A. Wakamiya, Y. Murata, and C. Adachi, *Nat. Commun.* 6, 8476 (2015).
4. D.R. Lee, B.S. Kim, C.W. Lee, Y. Im, K.S. Yook, S.-H. Hwang, and J.Y. Lee, *ACS Appl. Mater. Interfaces* 7, 9625 (2015).
5. C.H. Lee and J.Y. Lee, *Adv. Mater.* 25, 5450 (2013).
6. H. Sasabe and J. Kido, *Eur. J. Org. Chem.* 2013, 7653 (2013).
7. J.-H. Jou, Y.-T. Su, S.-H. Liu, Z.-K. He, S. Sahoo, H.-H. Yu, S.-Z. Chen, C.-W. Wang, and J.-R. Lee, *J. Mater. Chem. C* 4, 6070 (2016).
8. C. Sekine, Y. Tsubata, T. Yamada, M. Kitano, and S. Doi, *Sci. Technol. Adv. Mater.* 15, 034203 (2014).
9. F. Xua, H.U. Kima, J.-H. Kima, B.J. Jung, A.C. Grimsdale, and D.-H. Hwang, *Prog. Polym. Sci.* 47, 92 (2015).

10. C.A. Zuniga, S. Barlow, and S.R. Marder, *Chem. Mater.* 23, 658 (2011).
11. F. Dumur, *Org. Electron.* 25, 345 (2015).
12. J.H. Burroughes, D.D.C. Bradley, A.R. Brown, R.N. Marks, K. Mackay, R.H. Friend, R.L. Burns, and A.B. Holmes, *Nature* 347, 539 (1990).
13. G. Gustafsson, Y. Cao, G.M. Treacy, F. Klavetter, N. Colaner, and A.J. Heeger, *Nature* 357, 477 (1992).
14. S.-A. Chen, H.-H. Lu, and C.-W. Huang, *Polyfluorenes*, ed. U. Scherf and D. Neher (Berlin: Springer, 2008), p. 49.
15. M. Leclerc, *J. Poly. Sci. Part A Poly. Chem.* 39, 2867 (2001).
16. C. Zhu, L. Liu, Q. Yang, F. Lv, and S. Wang, *Chem. Rev.* 112, 4687 (2012).
17. Z. Ma, J. Ding, B. Zhang, C. Mei, Y. Cheng, Z. Xie, L. Wang, X. Jing, and F. Wang, *Adv. Funct. Mater.* 20, 138 (2010).
18. Z. Ma, J. Ding, Y. Cheng, Z. Xie, L. Wang, X. Jing, and F. Wang, *Polymer* 52, 2189 (2011).
19. D. Sun, X. Zhou, J. Liu, X. Sun, H. Li, Z. Ren, D. Ma, M.R. Bryce, and S. Yan, *ACS Appl. Mater. Interfaces* 7, 27989 (2015).
20. X. He, D. Cai, D.-Y. Kang, W. Haske, Y. Zhang, C.A. Zuniga, B.H. Wunsch, S. Barlow, J. Leisen, D. Bucknall, B. Kippelen, and S.R. Marder, *J. Mater. Chem. C* 2, 6743 (2014).
21. Z. Ren, R.S. Nobuyasu, F.B. Dias, A.P. Monkman, S. Yan, and M.R. Bryce, *Macromolecules* 49, 5452 (2016).
22. M.A. Baldo, D.F. O'Brien, Y. You, A. Shoustikov, S. Sible, M.E. Thompson, and S.R. Forrest, *Nature* 395, 151 (1998).
23. Y. Tao, C. Yang, and J. Qin, *Chem. Soc. Rev.* 40, 2943 (2011).
24. B. Minaev, G. Baryshnikov, and H. Agren, *Phys. Chem. Chem. Phys.* 16, 1719 (2014).
25. K.-H. Kim, S. Lee, C.-K. Moon, S.-Y. Kim, Y.-S. Park, J.-H. Lee, J.W. Lee, J. Huh, Y. You, and J.-J. Kim, *Nat. Commun.* 5, 4769 (2014).
26. W.Y. Lai, J.W. Levell, A.C. Jackson, S.-C. Lo, P.V. Bernhardt, I.D.W. Samuel, and P.L. Burn, *Macromolecules* 43, 6986 (2010).
27. J.W. Levell, J.P. Gunning, P.L. Burn, J. Robertson, and I.D.W. Samuel, *Org. Electron.* 11, 1561 (2010).
28. W.Y. Lai, J.W. Levell, P.L. Burn, S.-C. Lo, and I.D.W. Samuel, *J. Mater. Chem.* 19, 4952 (2009).
29. J.W. Levell, W.Y. Lai, R.J. Borthwick, S.-C. Lo, P.L. Burn, and I.D.W. Samuel, *J. Phys. Chem. C* 115, 25464 (2011).
30. J.W. Levell, W.-Y. Lai, R.J. Borthwick, P.L. Burn, S.-C. Lo, and I.D.W. Samuel, *New J. Chem.* 36, 407 (2012).
31. W.-Y. Lai, J.W. Levell, M.N. Balfour, P.L. Burn, S.-C. Lo, and I.D.W. Samuel, *Polym. Chem.* 3, 734 (2012).
32. W.-Y. Lai, M.N. Balfour, J.W. Levell, A.K. Bansal, P.L. Burn, S.-C. Lo, and I.D.W. Samuel, *Macromolecules* 45, 2963 (2012).
33. A. Menon, H. Dong, Z.I. Niazimbetova, L.J. Rothberg, and M.E. Galvin, *Chem. Mater.* 14, 3668 (2002).
34. S.J. Konezny, L.J. Rothberg, M.E. Galvin, and D.L. Smith, *Appl. Phys. Lett.* 97, 143305 (2010).
35. Z.A. Page, C.-Y. Chiu, B. Narupai, D.S. Laitar, S. Mukhopadhyay, A. Sokolov, Z.M. Hudson, R.B. Zerdan, A.J. McGrath, J.W. Kramer, B.E. Barton, and C.J. Hawker, *ACS Photonics* 4, 631 (2017).
36. F. Dumur, Y. Guillaneuf, A. Guerlin, G. Wantz, D. Bertin, F. Miomandre, G. Clavier, D. Gigmes, and C.R. Mayer, *Macromol. Chem. Phys.* 212, 1616 (2011).
37. R.D. Costa, E. Ortí, H.J. Bolink, S. Graber, C.E. Housecroft, and E.C. Constable, *J. Am. Chem. Soc.* 132, 5978 (2010).
38. R.D. Costa, E. Ortí, H.J. Bolink, F. Monti, G. Accorsi, and N. Armaroli, *Angew. Chem. Int. Ed.* 51, 8178 (2012).
39. S.B. Meier, D. Tordera, A. Pertegás, C. Roldán-Carmon, E. Ortí, and H.J. Bolink, *Mater. Today* 17, 217 (2014).
40. M.Y. Wong, M.-G. La-Placa, A. Pertegás, H.J. Bolink, and E. Zysman-Colman, *J. Mater. Chem. C* 5, 1699 (2017).
41. N. Armaroli, G. Accorsi, M. Holler, O. Moudam, J.-F. Nierengarten, Z. Zhou, R.T. Wegh, and R. Welter, *Adv. Mater.* 18, 1313 (2006).
42. S. Shao, J. Ding, L. Wang, X. Jinga, and F. Wang, *J. Mater. Chem.* 22, 24848 (2012).
43. S. Shao, J. Ding, L. Wang, X. Jinga, and F. Wang, *J. Am. Chem. Soc.* 134, 15189 (2012).
44. S. Shao, J. Ding, L. Wang, X. Jinga, and F. Wang, *J. Am. Chem. Soc.* 134, 20290 (2012).
45. J.H. Park, T.-W. Koh, J. Chung, S.H. Park, M. Eo, Y. Do, S. Yoo, and M.H. Lee, *Macromolecules* 46, 674 (2013).
46. D.A. Poulsen, B.J. Kim, B. Ma, C.S. Zonte, and J.M.J. Fréchet, *Adv. Mater.* 22, 77 (2010).
47. S.-C. Lo and P.L. Burn, *Chem. Rev.* 107, 1097 (2007).
48. P.L. Burn, S.-C. Lo, and I.D.W. Samuel, *Adv. Mater.* 19, 1675 (2007).
49. D.Y. Kondakov, *Dig. Tech. Pap. Soc. Inf. Disp. Int. Symp.* 39, 617 (2008).
50. E. Kozma, W. Mróz, F. Villafiorita-Monteleone, F. Galeotti, A. Andicsová-Eckstein, M. Catellania, and C. Botta, *RSC Adv.* 6, 61175 (2016).
51. E. Kozma, W. Mróz, and F. Galeotti, *Dyes Pigments* 114, 138 (2015).
52. J. Wang and L.M. Leung, *Dyes Pigments* 99, 105 (2013).
53. M.-H. Ho, M.-T. Hsieh, K.-H. Lin, T.-M. Chen, J.-F. Chen, and C.-H. Chen, *Appl. Phys. Lett.* 94, 023306 (2009).
54. J. Wang, L.M. Leung, S.-K. So, and C.Y.H. Chan, *Polym. Int.* 63, 363 (2014).
55. J. Shi and C.W. Tang, *Appl. Phys. Lett.* 80, 3201 (2002).
56. L. Qian, D. Bera, and P.H. Holloway, *J. Chem. Phys.* 127, 244707 (2007).
57. S.B. Lee, K.H. Park, C.W. Joo, J.-I. Lee, J. Lee, and Y.-H. Kim, *Dyes Pigments* 128, 19 (2016).
58. T.M. Figueira-Duarte and K. Müllen, *Chem. Rev.* 111, 7260 (2011).
59. D. Chercka, S.-J. Yoo, M. Baumgarten, J.-J. Kim, and K. Müllen, *J. Mater. Chem. C* 2, 9083 (2014).
60. G. Mallesham, C. Swetha, S. Niveditha, M.E. Mohanty, N.J. Babu, A. Kumar, K. Bhanuprakash, and V.J. Rao, *J. Mater. Chem. C* 3, 1208 (2015).
61. J. Wang, L.M. Leung, S.K. So, C.Y.H. Chan, and M.Y. Wong, *Polym. Int.* 63, 1797 (2014).
62. I. Natori, S. Natori, H. Sekikawa, and K. Ogino, *Polym. J.* 42, 875 (2010).
63. A. Botta, S. Pragliola, V. Venditto, A. Rubino, S. Aprano, A.D.G.D. Mauro, M.G. Maglione, and C. Minarini, *Polym. Compos.* 36, 1110 (2015).
64. A. Cappelli, V. Razzano, G. Fabio, M. Paolino, G. Grisci, G. Giuliani, A. Donati, R. Mendichi, W. Mróz, F. Villafiorita-Monteleone, and C. Botta, *RSC Adv.* 5, 101377 (2015).
65. M.Y. Wong and L.M. Leung, *New J. Chem.* 41, 512 (2017).
66. T. Nakano, T. Yade, M. Yokoyama, and N. Nagayama, *Chem. Lett.* 33, 296 (2004).
67. T. Nakano, *Polym. J.* 42, 103 (2010).
68. H. Li, Z. Wang, C. Song, Y. Wang, Z. Lin, J. Xiao, R. Chen, C. Zheng, and W. Huang, *J. Mater. Chem. C* 2, 6946 (2014).
69. M.Y. Wong and E. Zysman-Colman, *Adv. Mater.* 29, 1605444 (2017).
70. Y. Tao, K. Yuan, T. Chen, P. Xu, H. Li, R. Chen, C. Zheng, L. Zhang, and W. Huang, *Adv. Mater.* 26, 7931 (2014).
71. H. Uoyama, K. Goushi, K. Shizu, H. Nomura, and C. Adachi, *Nature* 492, 234 (2012).
72. Z. Yang, Z. Mao, Z. Xie, Y. Zhang, S. Liu, J. Zhao, J. Xu, Z. Chi, and M.P. Aldred, *Chem. Soc. Rev.* 46, 915 (2017).
73. M.Y. Wong, G.J. Hedley, G. Xie, L.S. Kölln, I.D.W. Samuel, A. Pertegás, H.J. Bolink, and E. Zysman-Colman, *Chem. Mater.* 27, 6535 (2015).
74. Y.J. Cho, B.D. Chin, S.K. Jeon, and J.Y. Lee, *Adv. Funct. Mater.* 25, 6786 (2015).
75. Y.J. Cho, K.S. Yook, and J.Y. Lee, *Adv. Mater.* 26, 6642 (2014).
76. A. Endo, K. Sato, K. Yoshimura, T. Kai, A. Kawada, H. Miyazaki, and C. Adachi, *Appl. Phys. Lett.* 98, 083302 (2011).
77. A.E. Nikolaenko, M. Cass, F. Bourcet, D. Mohamad, and M. Roberts, *Adv. Mater.* 27, 7236 (2015).

78. K. Shizu, M. Uejima, H. Nomura, T. Sato, K. Tanaka, H. Kaji, and C. Adachi, *Phys. Rev. Applied* 3, 014001 (2015).

79. S.A. Bagnich, S. Athanasopoulos, A. Rudnick, P. Schroegel, I. Bauer, N.C. Greenham, P. Strohriegl, and A. Köhler, *J. Phys. Chem. C* 119, 2380 (2015).

80. R.S. Nobuyasu, Z. Ren, G.C. Griffiths, A.S. Batsanov, P. Data, S. Yan, A.P. Monkman, M.R. Bryce, and F.B. Dias, *Adv. Optical Mater.* 4, 597 (2016).

81. K. Shizu, H. Noda, H. Tanaka, M. Taneda, M. Uejima, T. Sato, K. Tanaka, H. Kaji, and C. Adachi, *J. Phys. Chem. C* 119, 26283 (2015).

82. A.P. Monkman, H.D. Burrows, I. Hamblett, S. Navarathnam, M. Svensson, and M.R. Andersson, *J. Chem. Phys.* 115, 9046 (2001).

83. G. Xie, J. Luo, M. Huang, T. Chen, K. Wu, S. Gong, and C. Yang, *Adv. Mater.* 29, 1604223 (2017).

84. J. Luo, G. Xie, S. Gong, T. Chen, and C. Yang, *Chem. Commun.* 52, 2292 (2016).

85. S.Y. Lee, T. Yasuda, H. Komiyama, J. Lee, and C. Adachi, *Adv. Mater.* 28, 4019 (2016).

86. Y. Zhu, Y. Zhang, B. Yao, Y. Wang, Z. Zhang, H. Zhan, B. Zhang, Z. Xie, Y. Wang, and Y. Cheng, *Macromolecules* 49, 4373 (2016).

87. P. Chen, D. Yuan, L. Niu, C. Gao, and Z. Xiong, *Org. Electron.* 41, 100 (2017).

88. W. Wei, P. Kleine, Y. Karpov, X. Qiu, H. Komber, K. Sahre, A. Kiriy, R. Lygaitis, S. Lenk, S. Reineke, and B. Voit, *Adv. Funct. Mater.* 27, 1605051 (2017).

89. S. Ho, S. Liu, Y. Chen, F. So, and J. Photon, *Energy* 5, 057611 (2015).

90. H. Zheng, Y. Zheng, N. Liu, N. Ai, Q. Wang, S. Wu, J. Zhou, D. Hu, S. Yu, S. Han, W. Xu, C. Luo, Y. Meng, Z. Jiang, Y. Chen, D. Li, F. Huang, J. Wang, J. Peng, and Y. Cao, *Nat. Commun.* 4, 1971 (2013).

91. K. Sun, X. Xie, Y. Liu, W. Jiang, X. Ban, B. Huang, and Y. Sun, *J. Mater. Chem. C* 4, 8973 (2016).

92. L. Derue, S. Olivier, D. Tondelier, T. Maindron, B. Geffroy, and E. Ishow, *ACS Appl. Mater. Interfaces* 8, 16207 (2016).

93. G. Liaptsis, D. Hertel, and K. Meerholz, *Angew. Chem. Int. Ed.* 52, 9563 (2013).

94. Y.-J. Pu, T. Chiba, K. Ideta, S. Takahashi, N. Aizawa, T. Hikichi, and J. Kido, *Adv. Mater.* 27, 1327 (2015).

95. P.K.H. Ho, J.-S. Kim, J.H. Burroughes, H. Becker, S.F.Y. Li, T.M. Brown, F. Cacialli, and R.H. Friend, *Nature* 404, 481 (2000).

96. X. Yang, D.C. Müller, D. Neher, and K. Meerholz, *Adv. Mater.* 18, 948 (2006).

97. S. Wu, M. Aonuma, Q. Zhang, S. Huang, T. Nakagawa, K. Kuwabara, and C. Adachi, *J. Mater. Chem. C* 2, 421 (2014).

98. H. Gao, D.A. Poulsen, B. Ma, D.A. Unruh, X. Zhao, J.E. Millstone, and J.M.J. Fréchet, *Nano Lett.* 10, 1440 (2010).

99. H. Wettacha, S.S. Jester, A. Colsmann, U. Lemmer, N. Rehmann, K. Meerholz, and S. Höger, *Synth. Met.* 160, 691 (2010).

100. G. Xie, X. Li, D. Chen, Z. Wang, X. Cai, D. Chen, Y. Li, K. Liu, Y. Cao, and S.-J. Su, *Adv. Mater.* 28, 181 (2016).

101. Y. Xiang, S. Gong, Y. Zhao, X. Yin, J. Luo, K. Wu, Z. Lu, and C. Yang, *J. Mater. Chem. C* 4, 9998 (2016).

102. T. Nakagawa, S.-Y. Ku, K.-T. Wong, and C. Adachi, *Chem. Commun.* 48, 9580 (2012).

103. S. Nau, N. Schulte, S. Winkler, J. Frisch, A. Vollmer, N. Koch, S. Sax, and E.J.W. List, *Adv. Mater.* 25, 4420 (2013).

104. L.V. Kayser, M. Vollmer, M. Welnhofer, H. Krikcziokat, K. Meerholz, and B.A. Arndtsen, *J. Am. Chem. Soc.* 138, 10516 (2016).

105. C.A. Young, S. Saowsupa, A. Hammack, A.A. Tangonan, P. Anuragudom, H. Jia, A.C. Jamison, S. Panichphant, B.E. Gnade, and T.R. Lee, *J. Appl. Polym. Sci.* 131, 41162 (2014).

106. J.H. Cook, J. Santos, H. Li, H.A. Al-Attar, M.R. Bryce, and A.P. Monkman, *J. Mater. Chem. C* 2, 5587 (2014).

107. J.H. Cook, J. Santos, H. Li, H.A. Al-Attar, M.R. Bryce, and A.P. Monkman, *J. Mater. Chem. C* 3, 9664 (2015).

108. Z. Geng, G. Sato, K. Marumoto, and M. Kijima, *J. Poly. Sci. Part A Poly. Chem.* 54, 3454 (2016).

109. T.T. Steckler, O. Fenwick, T. Lockwood, M.R. Andersson, and F. Cacialli, *Macromol. Rapid Commun.* 34, 990 (2013).

110. J.J. Intemann, E.S. Hellerich, B.C. Tlach, M.D. Ewan, C.A. Barnes, A. Bhuwalka, M. Cai, J. Shinar, R. Shinar, and M. Jeffries-EL, *Macromolecules* 45, 6888 (2012).

111. I. Osken, A.S. Gundogan, E. Tekin, M.S. Eroglu, and T. Ozturk, *Macromolecules* 46, 9202 (2013).

112. J.J. McDowell, D. Gao, D.S. Seferos, and G. Ozin, *Polym. Chem.* 6, 3781 (2015).

113. U. Giovanella, C. Botta, F. Galeotti, B. Vercelli, S. Battiatoc, and M. Pasini, *J. Mater. Chem. C* 1, 5322 (2013).

114. W. Lu, J. Kuwabara, T. Iijima, H. Higashimura, H. Hayashi, and T. Kanbara, *Macromolecules* 45, 4128 (2012).

115. T. Guo, W. Zhong, A. Zhang, J. Zou, L. Ying, W. Yang, and J. Peng, *New J. Chem.* 40, 179 (2016).

116. F. Xu, J.-H. Kim, H.U. Kim, J.-H. Jang, K.Y. Yook, J.Y. Lee, and D.-H. Hwang, *Macromolecules* 47, 7397 (2014).

117. J. Sun, H. Wang, H. Xu, T. Zhang, L. Li, J. Li, Y. Wu, B. Xu, X. Zhang, and W. Lai, *Dyes Pigments* 130, 191 (2016).

118. J. Zhao, M. Lian, Y. Yu, X. Yan, X. Xu, X. Yang, G. Zhou, and Z. Wu, *Macromol. Rapid Commun.* 36, 71 (2015).

119. Z. Ma, L. Chen, J. Ding, L. Wang, X. Jing, and F. Wang, *Adv. Mater.* 23, 3726 (2011).

120. H. Tan, J. Yu, Y. Wang, J. Li, J. Cui, J. Luo, D. Shi, K. Chen, Y. Liu, K. Nie, and W. Zhu, *J. Poly. Sci. Part A Poly. Chem.* 50, 149 (2012).

121. E. Ravindran, S.J. Ananthakrishnan, E. Varathan, V. Subramanian, and N. Somanathan, *J. Mater. Chem. C* 3, 4359 (2015).

122. E. Ravindran, E. Varathan, V. Subramanian, and N. Somanathan, *J. Mater. Chem. C* 4, 8024 (2016).

123. M. Nagai, *ECS J. Solid State Sci. Technol.* 2, R218 (2013).

124. R. Noriega, J. Rivnay, K. Vandewal, F.P.V. Koch, N. Stingelin, P. Smith, M.F. Toney, and A. Salleo, *Nat. Mater.* 12, 1038 (2013).

125. H.A. Al-Attar and A.P. Monkman, *J. Appl. Phys.* 109, 074516 (2011).

126. Z.A. Kösemen, A. Kösemen, S. Öztürk, B. Canimkurbey, S.E. Sana, Y. Yerli, and A.V. Tunç, *Microelectron. Eng.* 161, 36 (2016).

127. A.V. Tunc, B. Ecker, Z. Dogruyol, S. Jüchter, A.L. Ugur, A. Erdogmus, S.E. San, J. Parisi, and E.V. Hauff, *J. Polym. Sci., Part B: Polym. Phys.* 50, 117 (2012).

128. G. Moad, E. Rizzardo, and S.H. Thang, *Acc. Chem. Res.* 41, 1133 (2008).

129. K. Matyjaszewski, *Macromolecules* 45, 4015 (2012).

130. T. Bura, T. Blaskovits, and M. Leclerc, *J. Am. Chem. Soc.* 138, 10056 (2016).

131. J.-R. Pouliot, F. Grenier, T. Blaskovits, S. Beaupré, and M. Leclerc, *Chem. Rev.* 116, 14225 (2016).

132. P. Bujak, I. Kulszewicz-Bajer, M. Zagorska, V. Maurel, I. Wielgusa, and A. Pron, *Chem. Soc. Rev.* 42, 8895 (2013).

133. Y. Lee and E.D. Gomez, *Macromolecules* 48, 7385 (2015).

134. R. Hu, N.L.C. Leung, and B.Z. Tang, *Chem. Soc. Rev.* 43, 4494 (2014).

135. Y. Hong, J.W.Y. Lam, and B.Z. Tang, *Chem. Soc. Rev.* 40, 5361 (2011).

136. S. Liu, C. Peng, A. Cruz, Y. Chen, and F. So, *J. Mater. Chem. C* 4, 8696 (2016).

137. H. Becker, I. Bach, M. Holbach, J. Schwaiger, and H. Spreitzer, *Dig. Tech. Pap. Soc. Inf. Disp. Int. Symp.* 41, 39 (2010).

138. C. Wang, X. Li, Y. Pan, S. Zhang, L. Yao, Q. Bai, W. Li, P. Lu, B. Yang, S. Su, and Y. Ma, *ACS Appl. Mater. Interfaces* 8, 3041 (2016).

139. H. Soofi and A. Rostami, *Jpn. J. Appl. Phys.* 54, 094301 (2015).

140. S.M. King, M. Cass, M. Pintani, C. Coward, F.B. Dias, A.P. Monkman, and M. Roberts, *J. Appl. Phys.* 109, 074502 (2011).

141. Y. Zhang, J. Lee, and S.R. Forrest, *Nat. Commun.* 5, 5008 (2014).